AGU PUBLICATIONS

Paleoceanography

RESEARCH ARTICLE
10.1002/2017PA003154

**Key Points:**
- The application of $\delta^{18}O$ data derived from *Glycymeris glycymeris* shells is evaluated as a new robust paleoceanographic proxy
- Subannual and annually resolved $\delta^{18}O$ data demonstrate significant skill at reconstructing NE Atlantic seawater temperature variability
- The $\delta^{18}O_{shell}$ record is sensitive to North Atlantic variability linked to changes in subpolar gyre dynamics and the North Atlantic Current

**Supporting Information:**
- Supporting Information S1

**Correspondence to:**
D. J. Reynolds,
reynoldsd3@cardiff.ac.uk

**Citation:**
Reynolds, D. J., Hall, I. R., Slater, S. M., Scourse, J. D., Halloran, P. R., & Sayer, M. D. J. (2017). Reconstructing past seasonal to multicentennial-scale variability in the NE Atlantic Ocean using the long-lived marine bivalve mollusk *Glycymeris glycymeris*. *Paleoceanography*, *32*. https://doi.org/10.1002/2017PA003154

Received 8 MAY 2017
Accepted 21 SEP 2017
Accepted article online 5 OCT 2017



# Reconstructing Past Seasonal to Multicentennial-Scale Variability in the NE Atlantic Ocean Using the Long-Lived Marine Bivalve Mollusk *Glycymeris glycymeris*

**D. J. Reynolds[1], I. R. Hall[1], S. M. Slater[1], J. D. Scourse[2], P. R. Halloran[3], and M. D. J. Sayer[4]**

[1]School of Earth and Ocean Sciences, Cardiff University, Cardiff, UK, [2]College of Life and Environmental Sciences, University of Exeter, Penryn, UK, [3]College of Life and Environmental Sciences, University of Exeter, Exeter, UK, [4]Natural Environment Research Council Facility for Scientific Diving, Scottish Association for Marine Science, Oban, UK

**Abstract** The lack of long-term, highly resolved (annual to subannual) and absolutely dated baseline records of marine variability extending beyond the instrumental period (last ~50–100 years) hinders our ability to develop a comprehensive understanding of the role the ocean plays in the climate system. Specifically, without such records, it remains difficult to fully quantify the range of natural climate variability mediated by the ocean and to robustly attribute recent changes to anthropogenic or natural drivers. Here we present a 211 year (1799–2010 C.E.; all dates hereafter are Common Era) seawater temperature (SWT) reconstruction from the northeast Atlantic Ocean derived from absolutely dated, annually resolved, oxygen isotope ratios recorded in the shell carbonate ($\delta^{18}O_{shell}$) of the long-lived marine bivalve mollusk *Glycymeris glycymeris*. The annual record was calibrated using subannually resolved $\delta^{18}O_{shell}$ values drilled from multiple shells covering the instrumental period. Calibration verification statistics and spatial correlation analyses indicate that the $\delta^{18}O_{shell}$ record contains significant skill at reconstructing Northeast Atlantic Ocean mean summer SWT variability associated with changes in subpolar gyre dynamics and the North Atlantic Current. Reconciling differences between the $\delta^{18}O_{shell}$ data and corresponding growth increment width chronology demonstrates that 68% of the variability in *G. glycymeris* shell growth can be explained by the combined influence of biological productivity and SWT variability. These data suggest that *G. glycymeris* can provide seasonal to multicentennial absolutely dated baseline records of past marine variability that will lead to the development of a quantitative understanding of the role the marine environment plays in the global climate system.

## 1. Introduction

North Atlantic seawater temperature (SWT) variability plays a significant role in the global climate system with the propagation of heat through the northward flowing surface currents (Gulf Stream/North Atlantic Current) acting as a "bottom-up" mechanism for driving atmospheric climate variability (Tandon & Kushner, 2015). Over the last glacial period there is ample evidence that abrupt fluctuations in North Atlantic SWTs, brought about by changes in ocean circulation patterns, were in part responsible for rapid high-amplitude fluctuations of ~5–10°C in Northern Hemisphere air temperatures (Heinrich and Dansgaard-Oeschger events; Broecker, 1998). However, the role that ocean variability plays in the modern climate system, where the magnitude of change is much smaller, is less well understood. Our current understanding is, in part, constrained by the short temporal, and spatially heterogeneous nature of modern observational records (Hurrell & Trenberth, 1999; Smith & Reynolds, 2004), the sparse distribution of subpolar coralline archives (e.g., Halfar et al., 2011; Kamenos, 2010), and the typically lower resolution (multidecadal) reconstructions from marine sediment cores that rely on radiocarbon ($^{14}C$) derived age models. While these latter sediment archives provide invaluable information regarding the amplitude and potential processes of past climate variability (e.g., Hall et al., 2010; Lund et al., 2006; Mjell et al., 2016; Moffa-Sánchez, Born, et al., 2014; Moffa-Sánchez, Hall, et al., 2014; Sicre et al., 2011), the large uncertainties associated with radiocarbon derived age models typically hinder the application of these data in resolving high-frequency (decadal to subdecadal) spatiotemporal variability and robustly assessing potential leads/lags within the marine system and in the ocean-atmosphere coupling.

The development of sclerochronological records, incorporating the analyses of the physical and geochemical variations in the accretionary skeletal tissues of aquatic, marine, and terrestrial organisms (e.g., Hudson et al.,

1976; Oschmann, 2009), provides the opportunity for the generation of absolutely dated and robustly calibrated reconstructions of past climate variability. Reconstructions derived from the analyses of marine bivalve growth increment width chronologies, constructed using dendrochronological cross-dating techniques (e.g., Butler et al., 2013; Jones, 1980; Jones et al., 1989; Marchitto et al., 2000), and stable isotope ($\delta^{18}O$ and $\delta^{13}C$; e.g., Reynolds et al., 2016; Schöne et al., 2005; Wanamaker et al., 2009, 2011; Witbaard et al., 1994) and radioisotope ($^{14}C$; Wanamaker et al., 2012) time series developed from long-lived marine bivalves, such as *Arctica islandica* and *Glycymeris glycymeris*, are now realized as robust archives of past marine variability. Hitherto, marine bivalve sclerochronological archives have provided robust reconstructions of past SWTs (Brocas et al., 2013; Mette et al., 2016; Reynolds et al., 2013, 2017; Schöne et al., 2004), oceanic carbon dynamics (Schöne et al., 2011), marine radiocarbon reservoir ages (Wanamaker et al., 2012), coupled ocean and terrestrial ecosystem dynamics (Black, 2009; Black et al., 2014; Helama et al., 2007) and to investigate the mechanisms and drivers of ocean variability (Lohmann & Schöne, 2013; Reynolds et al., 2016, 2017).

The ability to apply sclerochronological techniques to investigate past climate variability is, in part, controlled by the geographic distribution of suitable "target" species, which are spatially heterogeneous and dictated by their habitat preferences (e.g., SWT, salinity, seafloor sediment type, water depth, and the quality and quantity of food supply) among other factors. The study areas currently investigated are therefore a compromise between regions that are oceanographically and climatically sensitive and regions where there are abundant populations of the target species. To broaden the spectrum of environments that can be reconstructed, it is necessary to extend the range of species that can be utilized as past proxy archives. Previously, *A. islandica* has been considered the key archive for sclerochronological applications in the North Atlantic region. This is because of its exceptional longevity (>500 years, Butler et al., 2013) and the fact that shell growth is synchronous between individuals and populations, facilitating the use of cross-dating techniques developed by the dendrochronology community to be applied for constructing multicentennial to millennial length chronologies (Butler et al., 2013; Marchitto et al., 2000; Scourse et al., 2006; Witbaard et al., 1997). *Arctica islandica* aragonite shell also appears to faithfully record the $\delta^{18}O$ and $\delta^{13}C$ composition of the ambient waters bathing the animal during its lifetime (e.g., Reynolds et al., 2016; Schöne et al., 2005; Witbaard et al., 1994), and its shell is relatively simple to analyze for radiocarbon $^{14}C$ content (Scourse et al., 2012; Wanamaker et al., 2012).

The marine bivalve *Glycymeris glycymeris* (dog cockle or European bittersweet) has recently been identified as a potential target species and valuable sclerochronological archive in the North Atlantic region (Brocas et al., 2013; Reynolds, 2011; Reynolds et al., 2013; Royer et al., 2013). Similar to *A. islandica*, *G. glycymeris* has a multicentennial maximum longevity (~200 years; Reynolds et al., 2013), shells that consist of internal growth increments with an annual period (Berthou et al., 1986; Brocas et al., 2013; Royer et al., 2013) and the precipitation of aragonite (growth) occurs in synchrony between individuals and populations experiencing common environmental changes (Brocas et al., 2013; Reynolds et al., 2013). These characteristics are all important in facilitating the construction of robust chronologies extending back over many centuries (Brocas et al., 2013; Reynolds et al., 2013). Typically, *G. glycymeris* inhabits coarse seabed sediments (sand to gravel), characteristic of high-energy bottom environments, while *A. islandica* are more usually found in lower energy muddy to sandy environments (Hayward & Ryland, 1995). Absolutely dated chronologies constructed from *G. glycymeris* growth increment width series have been shown to be extremely sensitive to SWT variability allowing the direct reconstruction of past SWT variability from the growth increment series alone (Brocas et al., 2013; Reynolds et al., 2013). However, due to the limitations imposed by having to use statistical detrending techniques, necessary to remove the ontogenetic growth signal to enable the generation of the growth increment series, these reconstructions are typically insensitive to low-frequency variability, a problem recognized by the dendrochronology community as the "segment length curse" (Cook et al., 1995). The use of stable $\delta^{18}O_{shell}$ values from within individual growth increments could facilitate the application of *G. glycymeris* series for the reconstruction of past ocean variability across frequency domains. This is because no detrending is required in the construction of a $\delta^{18}O_{shell}$ series and the physical mechanisms that drive $\delta^{18}O$ variability in aragonite are relatively well understood (Schöne & Gillikin, 2013; Urey, 1948). However, up until now the application of *G. glycymeris* $\delta^{18}O_{shell}$ analyses as a proxy for seawater temperature (and or density), which has been widely used in *A. islandica* based studies, has yet to be fully investigated.

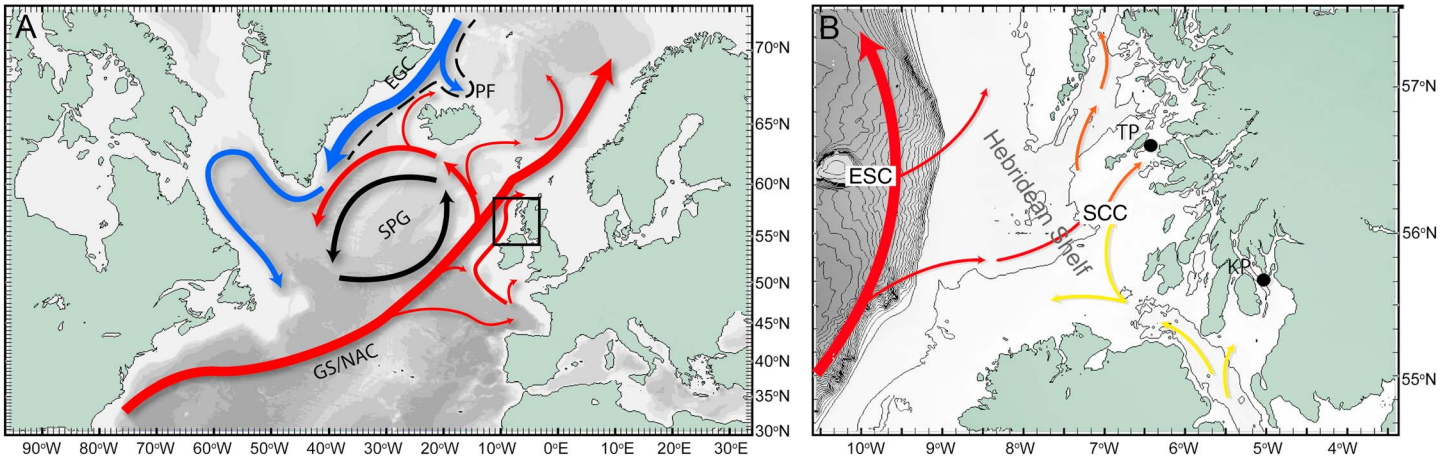


**Figure 1.** Map showing the major currents of (a) the North Atlantic and (b) the continental shelf of northwest Scotland. Shell samples were collected from the Tiree Passage (TP). Oceanographic data were obtained from oceanographic instrumental moorings at both Keppel Pier (KP) and TP. Red arrows denote warm saline currents, blue arrows represent cold fresh currents, and yellow and orange arrows denote coastal currents flowing north along the British coast. The black arrows denote the general circulation pattern of the subpolar gyre (SPG). Shaded contours spaced at 100 m depth intervals. GS/NAC = Gulf Stream/North Atlantic Current; EGC = East Greenland Current; PF = Polar Front; ESC = European Slope Current; SCC = Scottish Coastal Current. Figure adapted from Reynolds et al. (2016) and Inall et al. (2009).

The purpose of this study is therefore (1) to assess the timing and rate of subannual *G. glycymeris* shell growth to evaluate the likely seasonal bias in the annually resolved $\delta^{18}O_{shell}$ series, (2) to evaluate the potential application of $\delta^{18}O_{shell}$ series derived from *G. glycymeris* in reconstructing past ocean variability, (3) to evaluate the relative contribution of both salinity and SWTs in driving *G. glycymeris* $\delta^{18}O_{shell}$ variability, and (4) to robustly quantify the skill of the annually resolved $\delta^{18}O_{shell}$ data to reconstruct SWTs.

## 2. Oceanographic Setting

The *G. glycymeris* shell material examined in this study was collected from the Tiree Passage, located on the western fringes of the Hebridean continental shelf, northwest Scotland (56°37.75′N, 6°24.00′W; Figure 1). This locality is ideally situated for assessing the potential of *G. glycymeris* records as palaeoceanographic archives due to the proximity of two long-term instrumental oceanographic mooring data sets, in the Tiree Passage (Inall et al., 2009) and at Keppel Pier (55°44′55N, 4°54′20W; www.bodc.ac.uk/data/), as well as the abundance of both live and fossil specimens. The regional hydrography is dominated by the relative influence of the European Slope Current (ESC), which is a major branch of the North Atlantic Current (NAC), and the Scottish Coastal Current (SCC; Inall et al., 2009). Both the ESC and SCC are northward flowing currents advecting warm and salty Atlantic waters across the Hebridean shelf. However, the SCC waters, which form in the North Channel between Ireland and Scotland are slightly fresher than the ESC due to the influence of freshwater from riverine and precipitation inputs as Atlantic waters move northward through the Irish Sea and onto the Hebridean Shelf (Inall et al., 2009). Changes in the strength of the ESC have been investigated using satellite altimetry, tidal gauge, mooring observations, and conductivity-temperature-depth surveys and found to be associated with changes in broader Atlantic meridional overturning circulation (AMOC) strength, subpolar gyre (SPG) dynamics, and local wind stress (Holliday et al., 2015; Inall et al., 2009; Marsh et al., 2017; Xu et al., 2015). Given that the ESC dynamics are reflected in the physical and geochemical properties of the Sea of the Hebrides (Huthnance et al., 2009), developing long-term baseline records from this region could potentially provide information on the mechanisms and drivers of wider North Atlantic variability.

## 3. Methodology

### 3.1. Sample Collection

Live and dead (fossil) *G. glycymeris* shells were collected from the Tiree Passage (56°37.75′°N, 6°24.00′°W; Figure 1) using a mechanical dredge deployed by the *RV Prince Madog* in 2006 and via scuba diving by the UK Natural Environment Research Council Facility for Scientific Diving (NFSD) between 2011 and 2014. The shells were collected from water depths of between 25 and 55 m. Each of the shells sampled in this study

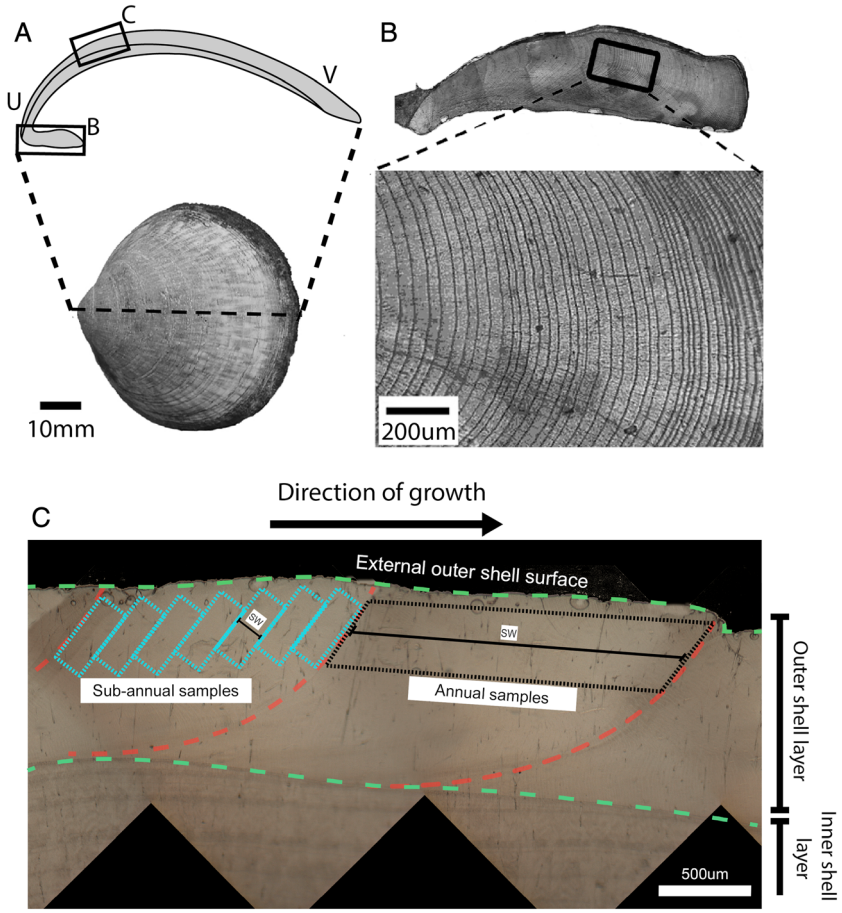


**Figure 2.** (a) Illustration demonstrating the line of section along the axis of maximum growth from the umbone to the ventral margin in a single *G. glycymeris* valve (dashed line on lower photograph) and the resulting cross section. U and V denote the positions of the umbone and the ventral margin portions of the shell, respectively. (b) A digital photomosaic of the tooth (enlargement of box B in plate A) and a single photomicrograph from the mosaic illustrating the clarity of the growth increment series in *G. glycymeris* shells. (c) The sampling strategy employed for microdrilling the annually and subannually resolved shell samples. The dashed red lines indicate the position of the annual growth check; the dashed green lines indicate the position of the periostracum and boundary between the outer and inner shell layers. The dashed black and blue parallelograms indicate the idealized drilling position of the annual and subannually resolved samples, respectively. The black lines labeled SW denote the width of the drilled sample, with the annual samples this is equivalent to the width of the growth increment, while in the subannual samples is 150 μm. Figures 2a and 2b modified from Reynolds et al. (2013).

had been previously dated as part of the construction of the *G. glycymeris* growth increment width master sclerochronology (Reynolds et al., 2013). In the construction of the growth increment width chronology live and dead-collected *G. glycymeris* shells were cross-dated using standard dendrochronological techniques facilitating the absolute dating of each of the growth increments (Butler et al., 2010; Marchitto et al., 2000; Scourse et al., 2006; Witbaard et al., 1997). The ages of the shells were then independently validated by "range finder" accelerator mass spectrometry $^{14}C$ dating (Reynolds et al., 2013). The growth increment width chronology subsequently provided an absolutely dated temporal framework which facilitated the microdrilling of samples, and the generation of a $\delta^{18}O_{shell}$ series, of absolute known ages. Full details of the shell collection, cross dating and $^{14}C$ analyses are provided in Reynolds et al. (2013).

### 3.2. Stable Isotope Analysis

Each of the *G. glycymeris* shells examined in this study was prepared using the conventional shell embedding and sectioning methodologies (Brocas et al., 2013; Reynolds et al., 2013; Richardson, 2001). The shells were embedded into epoxy resin and sectioned along the axis of maximum growth from the ventral margin to the umbone (Figure 2). The cut shell sections were then polished using increasingly finer grades of carborundum grit paper (400–4,000 grade, equivalent grit size down to approximately 3 μm) and polished using a

neoprene cloth and a 3 μm diamond solution. Aragonite powder samples of between 10 μg and 400 μg were then drilled from the growth increments of a subset of shells that had been previously dated, by means of cross dating, into the master *G. glycymeris* sclerochronology. The samples were drilled using a 300 μm tungsten carbide drill bit coupled to a Merchantek (New Wave) micromill system. This system permits visualization of the growth increments prior to drilling through a digital camera system embedded in the micromill facilitating the robust determination of the target growth increments (Figure 2). Shell samples were drilled using two strategies to facilitate the generation of ultrahigh-resolution subannual and annual resolution samples. Figure 2c provides a schematic of each of the sampling strategies employed. All the samples were drilled from the outer shell layer from the ventral margin to the umbone sections, rather than in the tooth, as this was the only region of the shell with growth increments of sufficient width for sampling.

For the subannual sampling, initially, a pit was drilled into the outer shell layer prior to the position of the first sampling location and the material discarded. The pit was required to remove aragonite material that was not in the target increment but would have otherwise been sampled due to the width of the drill bit (300 μm) being greater than the targeted sampling width (150 μm). Samples were then drilled using a sequential sampling strategy with each sample being 150 μm in width; the samples were drilled using between 10 and 15 passes each of 100 μm to provide a total sample swath of between 1 and 1.5 mm. The width of all subannually resolved samples was kept constant at 150 μm to facilitate the application of statistical techniques to assess seasonal changes in growth rates. Given that the growth increments vary in width from year to year, the subannual sampling methodology generated a mean of 13.7 (±3.7, 1$\sigma$) samples per year over the time interval from 1954 to 2010. The samples were drilled from a total of eight *G. glycymeris* shells.

For the annually resolved sampling, single samples were drilled from each growth increment. While the sample swath of each sample was kept constant (1 mm), the width of each sample was dictated by the width of the corresponding growth increment to ensure that each sample captured shell material spanning the entire period of the annual shell growth (black dashed parallelograms in Figure 2c). The drilling technique of using multiple passes, rather than drilling one deep line, ensured that the shell powder was thoroughly homogenized. This is particularly important for the annual samples as often the drilling process results in a large volume of material being collected, and therefore, only a subsample of the resulting material from each annual increment is actually analyzed for stable isotopes. We analyzed the $\delta^{18}O_{shell}$ composition of 107 replicate subsamples from 13 individual shells to assess the homogenization of the carbonate powder (1$\sigma$ = <0.10‰).

All carbonate samples were analyzed using a Kiel IV carbonate device coupled to a Thermo Finnigan MAT 253 mass spectrometer (Cardiff University). The shell carbonate samples were analyzed alongside internal standard Carrara marble (no less than six standards per 40 shell carbonate samples) and calibrated against NBS-19 international standard relative to Vienna Peedee belemnite (VPDB). The samples were analyzed using 100% orthophosphoric acid at 70°C for 300 s. To make our isotope data directly comparable to the Royer et al. (2013) G. glycymeris stable isotope study, which did not apply a phosphoric acid fractionation factor for calcite (Thebault pers. comm. 2017), we therefore did not apply a specific aragonite phosphoric acid fractionation factor (e.g., Kim et al., 2007) to our isotopic measurements. The external precision (1$\sigma$) for the $\delta^{18}O$ analyses, based on replicate measurements of laboratory reference sample (Carrera marble), was ≤0.05‰.

To test whether the modern $\delta^{18}O_{shell}$ data are significantly different to that occurring during the previous two centuries, the mean and standard deviation of the annually resolved $\delta^{18}O_{shell}$ data were calculated within discrete 10 year nonoverlapping bins. These data were tested for normality using the Shapiro-Wilk test. The independent sample (student) *t* test was then used to compare the mean $\delta^{18}O_{shell}$ values over the period from 2001 to 2010 (modern) with the 10 year binned data over the previous two centuries.

### 3.3. Seawater Temperature Calibration

The annual and subannual $\delta^{18}O_{shell}$ series were converted to SWTs using (i) the Grossman and Ku (1986) aragonite palaeotemperature equation (equation (1)) and (ii) the Royer et al. (2013) empirically derived *G. glycymeris* species-specific palaeotemperature equation (equation (2)). Both equations require the $\delta^{18}O$ of ambient seawater ($\delta^{18}O_{sw}$) to be known to convert the $\delta^{18}O_{shell}$ ratios into absolute SWTs. Over the instrumental period we applied the Cage and Austin (2010) local $\delta^{18}O_{sw}$ versus salinity mixing line equation (equation (3)) to estimate $\delta^{18}O_{sw}$ from the local observational seawater temperature and salinity time series.

As the Tiree Passage salinity record is relatively short (Inall et al., 2009) we also derived sea surface salinity (SSS) data from the EN4 gridded SSS data set (Good et al., 2013) estimated from a 10°× 10° grid box centered on the Tiree Passage. In both calibrations we subtracted 0.27‰ to convert the $\delta^{18}O_w$ values from Vienna Standard Mean Ocean Water (VSMOW) to Vienna Peedee belemnite (VPDB) scales (Hut, 1987). The reconstructed SWTs are hereafter referred to as $T\delta^{18}O_{shell}$.

$$T\delta^{18}O_{shell}(°C) = 20.60–4.34 \times \left(\delta^{18}O_{shell}(VPDB)–\left(\delta^{18}O_{w\ VSMOW}–0.27\right)\right) \quad (1)$$

$$T\delta^{18}O_{shell}(°C) = 18.11–2.66 \times \left(\delta^{18}O_{shell}(VPDB)–\left(\delta^{18}O_{w\ VSMOW}–0.27\right)\right) \quad (2)$$

$$\delta^{18}O_w = 0.18 \times \text{salinity}–6.00 \quad (3)$$

As there are currently no independent salinity or $\delta^{18}O_w$ records that extend beyond the modern instrumental period, from either the northeast Atlantic or on the Hebridean shelf, we adopted two approaches to quantify the associated salinity/$\delta^{18}O_w$ uncertainty on the corresponding $T\delta^{18}O_{shell}$ estimates. In the first approach we quantified the mean squared error (MSE) between two $T\delta^{18}O_{shell}$ series, over the time interval from 1954 to 2007, in which in one of the reconstructions the $\delta^{18}O_{sw}$ values were kept constant and the second reconstruction the $\delta^{18}O_{sw}$ values varied based on the conversion of EN4 SSS data to $\delta^{18}O_w$ values using equation (3). In the second approach, we quantified the difference between two $T\delta^{18}O_{shell}$ reconstructions generated using two constant salinities that are representative of (i) open ocean Atlantic water (salinity = 35.0) and (ii) surface coastal waters (salinity = 33.5). Though these differences reflect the maximum potential influence of salinity on the SWT reconstruction, such a high-amplitude change in salinity is highly unlikely at the shell sampling location in Tiree Passage.

Whereas oceanographic mooring data indicate that the Tiree Passage has a salinity of ~34.5, the more coastal locality of Keppel Pier has a salinity of ~33.5 (Inall et al., 2009). Therefore, in order to test the skill of $T\delta^{18}O_{shell}$ series for reconstructing Keppel Pier SWTs, we used (i) a constant salinity value of 33.5 and (ii) a variable salinity record (EN4 SSS; Good et al., 2013), which also has a mean of 33.5. The salinity of 33.5 was only used for the comparison of the $T\delta^{18}O_{shell}$ series against the Keppel Pier observations. For the final $T\delta^{18}O_{shell}$ reconstruction of SWTs in the Tiree Passage a salinity value of 34.5 was used. While varying the salinity constant does not change the structure of variability within the reconstruction, using the lower salinity of 33.5 would result in the $T\delta^{18}O_{shell}$ overestimating Tiree Passage SWTs, and so the more accurate local value of 34.5 was used.

To define the growing season of the *G. glycymeris* population in the Tiree Passage, the subannually resolved $T\delta^{18}O_{shell}$ data were compared against seasonal SWTs recorded from both Keppel Pier and Tiree Passage. The comparisons were made using both the Grossman and Ku (1986) and the Royer et al. (2013) paleotemperature equations to determine independent growing seasons. The monthly resolution of the instrumental SWT data restricts our ability to provide a complete assessment of whether the subannual growth rate of *G. glycymeris* is linear or nonlinear. However, to take potential variations in the rate of *G. glycymeris* seasonal growth into account, we applied both a linear and nonlinear growth rate model to assign calendar positions, within each absolutely dated growth increment, to the subannually resolved $T\delta^{18}O_{shell}$ data. Supporting information Figure S2 shows a schematic detailing the linear and nonlinear growth rate models applied. The linear and nonlinear growth rate models were also applied to generate weighted mean growing season instrumental SWT series that were used, in addition to arithmetic mean growing season and arithmetic mean summer (June to August) SWTs, as targets for the calibration of the annually resolved $T\delta^{18}O_{shell}$ data.

We adopted the standard dendrochronological and sclerochronological reduction of error (RE), coefficient of efficiency (CE), and percentage variance ($R^2$, North et al., 2000) statistical techniques for assessing the skill of the $T\delta^{18}O_{shell}$ series, generated using both the variable and constant salinity approaches together with both palaeotemperature equations, at reconstructing SWT variability in the instrumental SWT time series. The Keppel Pier SWT data set was used for this comparison rather than the Tiree Passage mooring data because, while the Tiree Passage mooring is more proximal to the shell collection site, the observation period of the data set is considerably shorter (1981–2006) and it is also discontinuous as it contains several annual gaps (Inall et al., 2009). In comparison, the Keppel Pier data set spans from 1953 to 2007 and provides a continuous monthly record of SWT data that despite being located around 150 km farther south than the Tiree Passage shell collection site has been shown to contain SWT variability that is coherent with the Tiree Passage (Reynolds et al., 2013). While the $R^2$ statistic provides an indication of the degree of variance replicated by

the target proxy series, the RE and CE statistics assess the sensitivity of the reconstruction relative to subtle shifts in the target variable mean between the independent calibration and verification periods (North et al., 2000). Given the duration of the Keppel Pier instrumental data set, we used the time intervals of 1980–2007 and 1954–1979 for the calibration and verification periods, respectively.

Spatial correlation analyses were conducted, using the KNMI Climate Explorer Facility (Trouet & Van Oldenborgh, 2013), between the $T\delta^{18}O_{shell}$ series and gridded environmental data sets over the calibration period. This period was used as it is the period represented by the satellite measurements providing the broadest coverage of instrumental data over the North Atlantic region while still providing sufficient data to provide a robust statistical test. Prior to this period the spatial coverage of instrumental data becomes increasingly sparse (Hurrell & Trenberth, 1999; Smith & Reynolds, 2004). Spatial correlations were calculated between the raw and linear detrended $T\delta^{18}O_{shell}$ series and HadISST1 gridded sea surface temperatures (SSTs; Rayner et al., 2003) and EN4 gridded SSS (Good et al., 2013). While it is important to assess the degree of coherence across all frequency domains, to account for the high degree of autocorrelation in both the $T\delta^{18}O_{shell}$ series and the instrumental data sets, which can lead to an overestimate of the significance of the correlation between the two series, we examined the correlations using both the raw nondetrended data and linear detrended data. Additionally, we applied the Ebisuzaki Monte Carlo bootstrapping methodology, which takes into account the degree of autocorrelation in each of the data sets, to provide a more robust assessment of the significance of the correlations (Ebisuzaki, 1997).

### 3.4. Multiproxy Analyses

The $T\delta^{18}O_{shell}$ series was compared with contemporaneous proxy archives from the Tiree Passage and adjacent Loch Sunart. For the comparison with the coregistered *G. glycymeris* growth increment width master sclerochronology, constructed from the same shells used to derive the $\delta^{18}O_{shell}$ series, the $T\delta^{18}O_{shell}$ data were also detrended using a 100 year first-order loess high-pass filter. This was necessary as the construction of the growth increment width chronology is based on detrended data, required to remove the biological growth trends (Schöne & Gillikin, 2013). In all other comparison no statistical detrending of the $\delta^{18}O_{shell}$ isotope record was used. The Loch Sunart $\delta^{18}O$, which is derived from the analysis of benthic foraminifera (Cage & Austin, 2010), was linear interpolated to annual resolution to facilitate a linear regression analysis to be performed against the $T\delta^{18}O_{shell}$ series. This interpolation was necessary as the Loch Sunart $\delta^{18}O$ series contains variable sampling resolution. Running correlation analysis was used to evaluate the stability of the correlation between the $T\delta^{18}O_{shell}$ series and the *G. glycymeris* growth increment width sclerochronology.

A multiple linear regression model was used to investigate the possibility that variability contained in the *G. glycymeris* growth increment width chronology is driven by the combined influence of variability in SWT and biological productivity (specifically primary productivity and zooplankton abundance). The analyses were conducted using the *R* statistics V3.47.1 package. The analyses were repeated three times, initially incorporating the Keppel Pier SST record and seasonal primary productivity (measured as the greenness of the water column and diatom abundance) and zooplankton abundance (measured as the abundance of copepods). The analyses were then repeated omitting the SST series to evaluate solely the coherence between the growth increment width chronology and primary productivity and zooplankton abundance. Finally, the model was run using only the measures of primary productivity. The primary productivity and zooplankton abundance data were obtained from the Continuous Plankton Recorder (CPR) survey data set from the grid box 55–60°N by 0–10°W (www.sahfos.ac.uk/DOI:10.7487/2017.216.1.1072).

## 4. Results

### 4.1. Raw Isotope Data

#### 4.1.1. Subannual $\delta^{18}O_{shell}$ Data

In total, we derived the $\delta^{18}O_{shell}$ values of 1,052 subannually resolved aragonite samples from the growth increments of eight independently sampled shells (Figure 3). The subannual data span the time interval from 1954 to 2010. The number of samples derived from each growth increment varied from 3 to 22 per year, with a mean 13.7 (±3.7, 1$\sigma$) samples per year. The number of samples per increment was variable due to the fixed width of the drilled samples (150 μm) and the highly variable width of the growth increments, resulting in the overall reduction in samples drilled from narrower growth increments. The subannual $\delta^{18}O_{shell}$ series shows a strong sinusoidal-like curve with values, across all increments, ranging from 0.84 to 2.64‰ (Figure 3). This

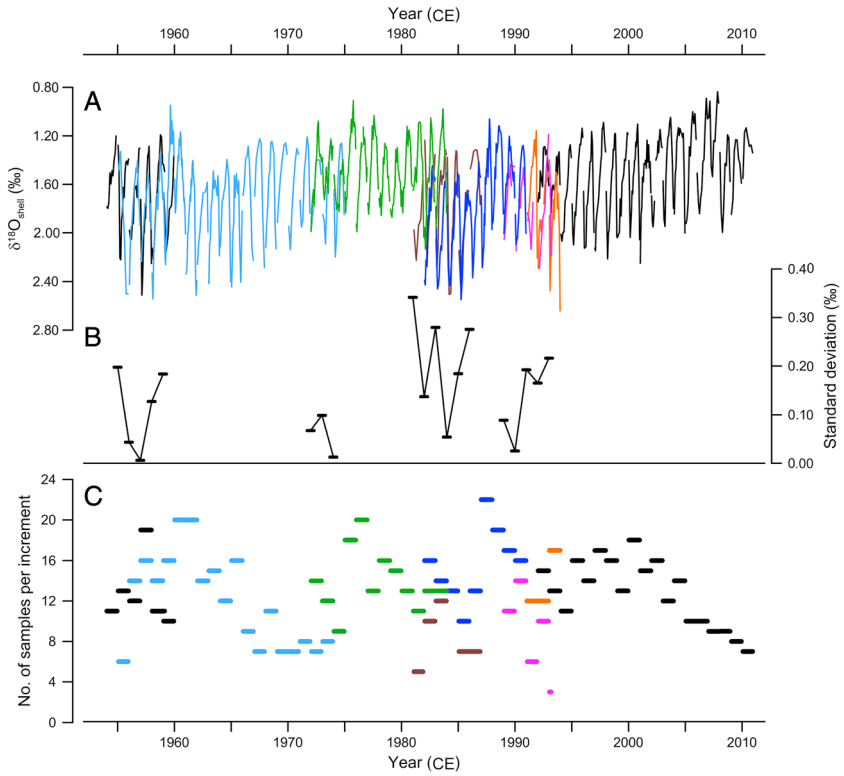


**Figure 3.** (a) Subannually resolved $\delta^{18}O_{shell}$ data plotted for each absolutely dated year sampled over the period from 1954 to 2010. The subannual data are plotted relative to sampling position within the growth increment and not based on a seasonal growth model. (b) Standard deviation calculated between $\delta^{18}O_{shell}$ data derived from the same year across multiple shells. (c) Number of independent samples analyzed per growth increment sampled. Different colored lines represent each individual shell sampled.

1.80‰ $\delta^{18}O_{shell}$ range equates to a SWT range of ~ 7.7°C, assuming a 4.3°C change in temperature per 1‰ in $\delta^{18}O$ and no influence of varying salinity.

As the sampling resolution of each increment was not constant, due to the variable width of the growth increments and the constant width of the drilled sample (150 μm), in order to quantify the offsets between shells and derive the intershell $\delta^{18}O$ and corresponding SWT uncertainty, the subannual isotopic values for each increment were arithmetically averaged to derive an annually resolved record for each shell. The standard deviation was then calculated between the $\delta^{18}O$ ratios in 19 years replicated across 41 increments in the eight sampled shells. These analyses indicated a 1$\sigma$ uncertainty of 0.14‰; this level of uncertainty equates to SWT uncertainty of ±0.6°C.

#### 4.1.2. Annually Resolved $\delta^{18}O_{shell}$ Data

We derived the $\delta^{18}O_{shell}$ values of 441 annually resolved aragonite samples from seven independently sampled *G. glycymeris* shells spanning the time interval from 1799 to 2010. Replicate samples drilled from growth increments representing the same years in multiple shells provide an assessment of the intershell variability (Figure 4). These replicates indicate an intershell variability (mean of the 1$\sigma$ standard deviation of the 396 replicates across the 181 replicated years) of ±0.12‰. This equates to a SWT uncertainty of ±0.5°C. The standard deviation of all the available replicated annually resolved increments, including the annual average of the subannual resolution $\delta^{18}O_{shell}$ data combined with the actual annually sampled $\delta^{18}O_{shell}$ data, provides a total estimate of the intershell variability. These data include a total of 473 independent growth increments representing 185 unique years and contain a 1$\sigma$ uncertainty of ±0.13‰, equivalent to a temperature uncertainty of ~±0.6°C.

The annually resolved $\delta^{18}O_{shell}$ series is characterized by two distinct intervals (Figure 5). From 1799 to ~1900–1910 the $\delta^{18}O_{shell}$ series contains an increasing trend, with the shells becoming heavier at a rate of +0.0025‰ $yr^{-1}$. Between 1890 and 1920 the $\delta^{18}O_{shell}$ remains stable at ~1.76 ± 0.09‰. However, over the

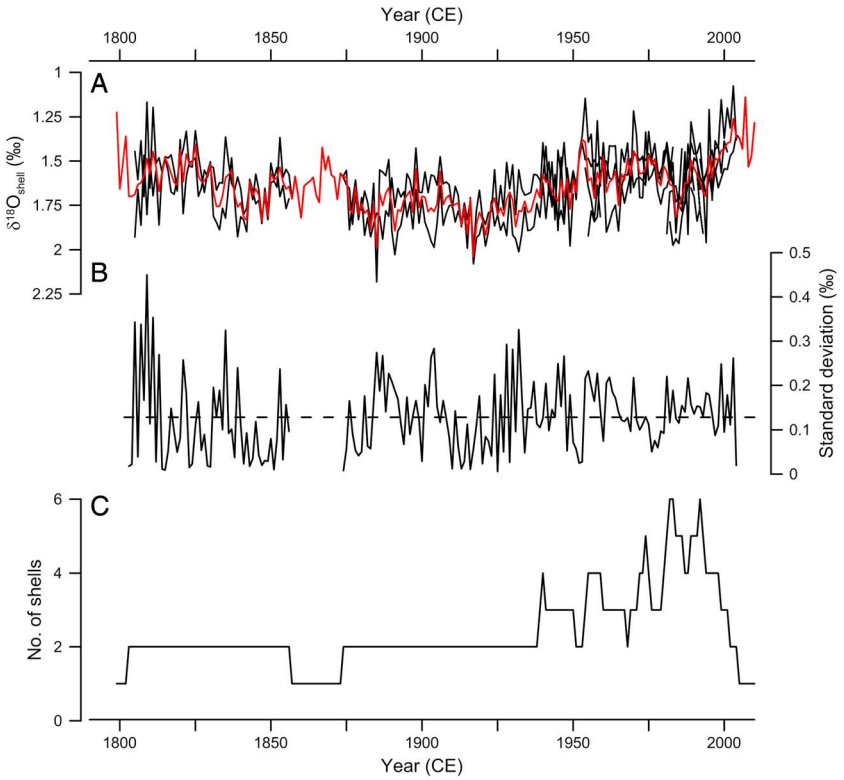


**Figure 4.** (a) Comparison between the annually resolved $\delta^{18}O_{shell}$ data, and the annual mean of the subannually resolved $\delta^{18}O_{shell}$ data, from all *G. glycymeris* shells independently sampled (black lines) with the mean $\delta^{18}O_{shell}$ series shown in red. (b) The solid black line shows the standard deviation of the $\delta^{18}O_{shell}$ data calculated between samples replicated between independent shells. The dashed black line denotes the mean standard deviation across all replicated years ($1\sigma = 0.13$‰). (c) Number of shells sampled in each given year.

time interval from 1920 to 2010, the 19th century trend in the $\delta^{18}O_{shell}$ series reverses with the shells gradually become lighter at a rate of $-0.004$‰ yr$^{-1}$. These long-term $\delta^{18}O_{shell}$ gradients equate to a cooling trend (assuming 4.3°C per 1‰ change in $\delta^{18}O_{shell}$) of ~0.10°C per decade over the 19th century and a warming trend of ~0.17°C per decade over the period from 1920 to 2010.

Examination of the decadal binned $\delta^{18}O_{shell}$ data (Figure 5), with zero years overlap between bins, indicates that the time interval of 2001–2010 as being significantly different to any other 10 year period over the reconstruction period from 1799 to 2010 ($P < 0.001$; for full student *t* test results see supporting information Table S1).

### 4.2. Environmental Analyses

#### 4.2.1. Subannual Data

The subannually resolved T$\delta^{18}O_{shell}$ data contain temperatures that range from 8.8 to 16.6°C and 9.3 to 16.2°C using the Grossman and Ku (1986) and the Royer et al. (2013) paleotemperature equations, respectively (Figures 6 and 7). Comparison of the subannually resolved T$\delta^{18}O_{shell}$ data with the seasonal SWT curves from both Keppel Pier and the Tiree Passage (Figure 6) as well as monthly HadISST1 SSTs (Figure 7), derived from a 10° × 10° grid box (50°–60°N 0°–10°W), demonstrates that T$\delta^{18}O_{shell}$ series corresponds to SWT over the period from May to October using the Grossman and Ku (1986) equation and from June to September using the Royer et al. (2013) equation (Figure 6). The T$\delta^{18}O_{shell}$ data, generated using both equations and applying both linear and nonlinear growth models, indicate that peak reconstructed temperatures are temporally synchronous and match in amplitude (within error) the peak summer SWTs in the monthly HadISST1 SSTs. None of the T$\delta^{18}O_{shell}$ data appear to match SWTs during the months of November to April (Figure 7).

#### 4.2.2. Annually Resolved Data

Significant positive correlations were identified between the T$\delta^{18}O_{shell}$ series, generated using both calibration equations and constant and variable approaches to salinity variability, and mean summer, arithmetic and

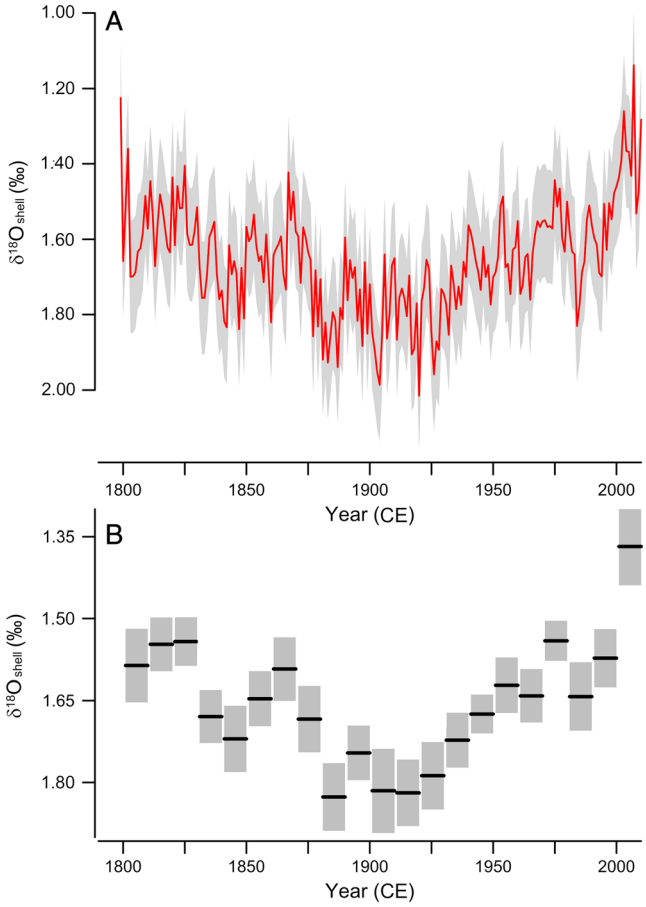


**Figure 5.** (a) Annually resolved $\delta^{18}O_{shell}$ data (red line) fitted with uncertainty envelope calculated using the sum of the intershell variability and external precision (shaded gray area). (b) Ten-year binned mean $\delta^{18}O_{shell}$ data (black lines), with zero years overlap between bins, fitted with 95% confidence intervals (shaded gray boxes).

weighted mean growing season SWTs (Table 1 and Figure 8). The $T\delta^{18}O_{shell}$ data generated using the Grossman and Ku (1986) equation explained between 29% and 49% of the variance in arithmetic mean summer SWT and 25% to 52% of the variance in mean growing season (May–October) SWT. The variable salinity approach to converting the $\delta^{18}O_{shell}$ data to SWTs contains marginally lower $R^2$ values against all three target parameters ($R^2$ = 0.36 to 0.52 compared to 0.25 to 0.50 for constant and variable salinity approaches, respectively). The $T\delta^{18}O_{shell}$ data generated using the Royer et al. (2013) equation explained between 29% and 49% of arithmetic mean summer SWT variance and 23% to 47% of the growing season (June–September) SWT variance. As with the Grossman and Ku derived $T\delta^{18}O_{shell}$ series the reconstructed temperatures derived using the Royer et al. (2013) equation using the variable salinity approach explain marginally less variance in the target parameters than those where the constant salinity was applied ($R^2$ = 0.35 to 0.49 compared to 0.23 to 0.47 for constant and variable salinity approaches, respectively).

The examination of the reconstructions MSE, RE, and CE statistics indicates that only the Grossman and Ku (1986)-based reconstructions of arithmetic mean summer SWT and weighted growing season SWT (using both approaches to salinity) contain significant skill (RE and CE $\geq$ 0, $P < 0.001$; Table 1). However, despite the significant Pearson correlation and RE statistics, the Grossman and Ku (1986)-based reconstructions of arithmetic mean growing season, using both approaches to salinity, do not contain significant CE statistics (CE $<$ 0). In contrast, while the Royer et al. (2013) derived $T\delta^{18}O_{shell}$ series performed well over the calibration period against all three target parameters, each of the reconstructions contains nonsignificant CE statistics (CE $<$ 0) over the verification period. The application of the Grossman and Ku (1986) aragonite paleotemperature equation with a constant salinity (34.5) therefore provides the robust reconstruction of weighted mean growing season SWTs over the last two centuries (Figure 9).

Examination of the spatial correlations calculated between the $T\delta^{18}O_{shell}$ series and the HadISST1 SST and EN4 SSS gridded data over the time interval 1980–2007 (Figure 10) indicates that the $T\delta^{18}O_{shell}$ series correlates with variability over broad regions of the North Atlantic. Highly significant positive correlations were identified with the raw (undetrended) HadISST1 SST data set over regions spanning from the equatorial Atlantic from the west coast of Africa to the Gulf of Mexico and tracking the trajectory of the southern, eastern, and northern boundary currents of the SPG including in the Labrador Sea. However, no significant correlations were identified with SSTs in the central region of the SPG. The spatial correlation patterns between the linear detrended $T\delta^{18}O_{shell}$ series and HadISST1 SSTs were constrained to the east and northern boundary currents of the SPG (Figure 10b). The spatial correlation analyses between the $T\delta^{18}O_{shell}$ series and EN4 gridded SSS data indicate no significant correlation with salinity on the Hebridean Shelf. However, the correlation analyses do indicate significant positive correlations with salinity variability in the Labrador Sea and in the central regions of the North Atlantic. The correlations with the Labrador Sea SSS are consistent using both the raw (undetrended) and linear detrended data sets, although are somewhat more spatially constrained using the linear detrended data (Figures 10c and 10d).

### 4.3. Multiproxy Analyses

Linear regression analyses identified a significant positive correlation between the $T\delta^{18}O_{shell}$ and the linear interpolated Loch Sunart benthic $\delta^{18}O$ series ($R$ = 0.23, $P < 0.05$, calculated over the period 1799–2001; Cage & Austin, 2010). However, examination of the coherence between the coregistered $T\delta^{18}O_{shell}$ series and the *G. glycymeris* growth increment width sclerochronology using 20 year running correlations indicates a variable relationship between shell growth and the $T\delta^{18}O_{shell}$ data (Figure 11). Over the instrumental period

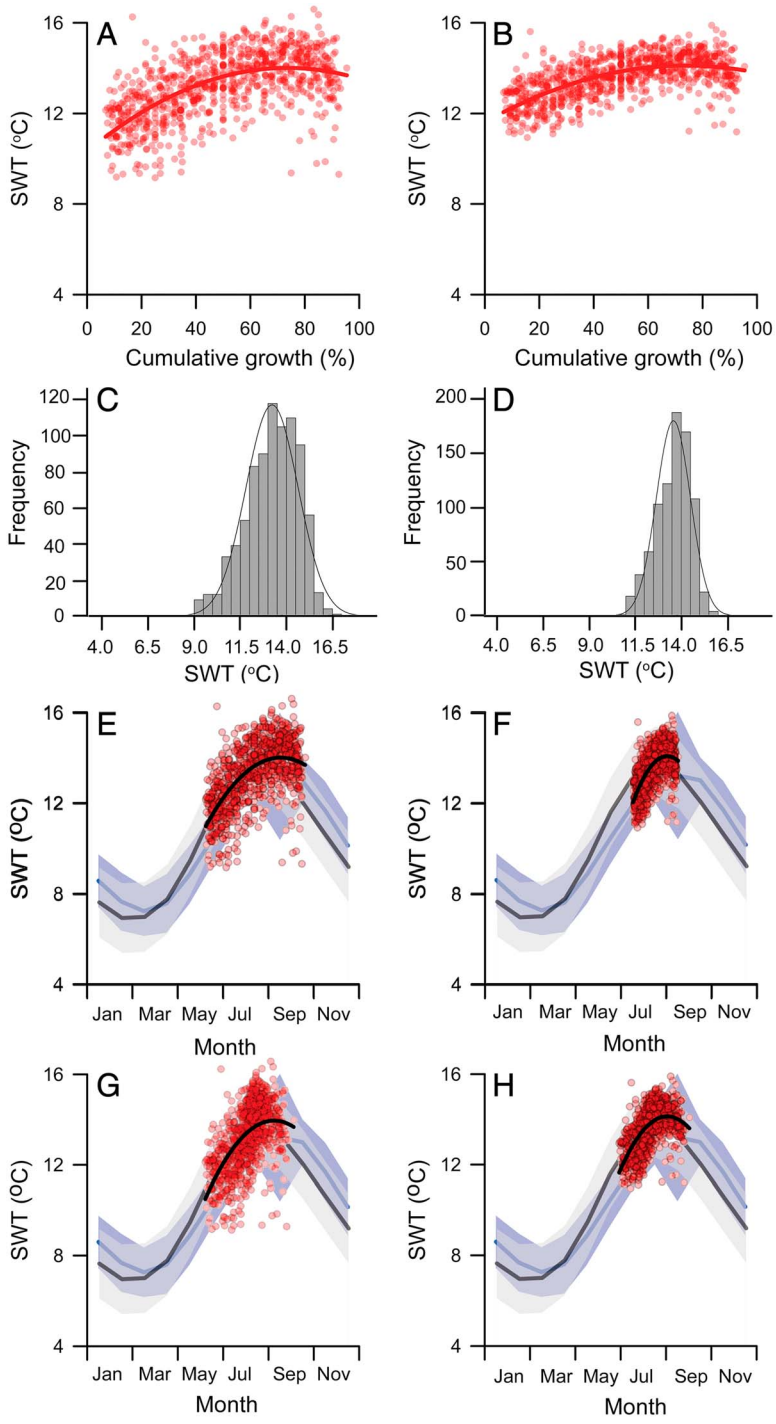


**Figure 6.** Comparison between the subannually resolved T$\delta^{18}O_{shell}$ data, calibrated using the Grossman and Ku (1986; plots A, C, and E) and Royer et al. (2013; plots B, D, and F) palaeotemperature equations, and mean seasonal SWTs recorded in the Keppel Pier and Tiree Passage instrumental time series. (a and b) Plot of the T$\delta^{18}O_{shell}$ data (red circles) plotted with respect to the relative sampling position (given as percentage of cumulative growth). The red line shows the polynomial best fit generated excluding the first and last sample of each increment. Supporting information Figure S1 shows all the subannually resolved data including the first and last sample from each increment. (c and d) Frequency histograms demonstrating the distribution of the subannually resolved T$\delta^{18}O_{shell}$ data. (e and f) Comparison between the subannual T$\delta^{18}O_{shell}$ data, plotted assuming linear seasonal growth, and (g and h) non-linear seasonal growth with the arithmetic mean ($\pm 2\sigma$) seasonal SWT curves from the Tiree Passage (blue line with shaded blue envelope) and Keppel Pier (black line with shaded gray envelope). For the comparison between T$\delta^{18}O_{shell}$ data plotted using linear and nonlinear growth models and seasonal SWTs see supporting information Figure S3.

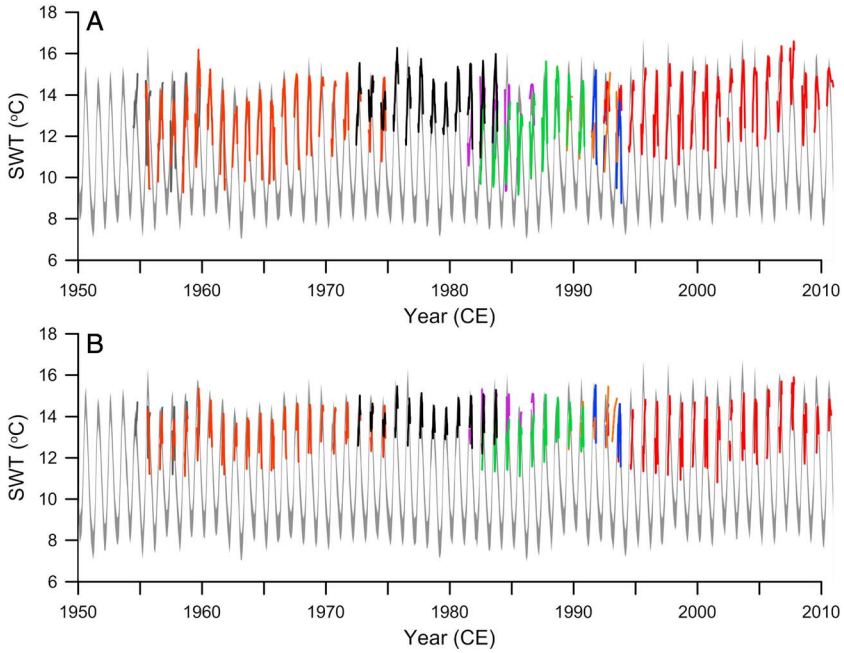


**Figure 7.** Subannually resolved $T\delta^{18}O_{shell}$ data generated using (a) the Grossman and Ku (1986) and (b) the Royer et al. (2013) paleotemperature equations, plotted against monthly HadISST1 SSTs (gray line) from a 10° × 10° grid box (50°–60°N 0°–10°W). Each shell sampled is represented with a different colored line. For the comparison between $T\delta^{18}O_{shell}$ data plotted using linear and nonlinear growth models and seasonal SWTs see supporting information Figure S3.

(1950–2000) and early 19th century the $T\delta^{18}O_{shell}$ data and *G. glycymeris* chronology exhibit positive correlations. However, during the late 19th and early 20th century the $T\delta^{18}O_{shell}$ series and *G. glycymeris* chronology exhibit negative to negligible coherence.

Significant correlations were identified between the *G. glycymeris* growth increment width sclerochronology and primary productivity on the Hebridean shelf ($R = 0.44$, $P < 0.1$, calculated over the period 1958–2010). The correlation between the *G. glycymeris* and zooplankton abundance was found to be nonsignificant

**Table 1**
*Comparison Between Pearson Correlation, Percentage Variance, Mean Squared Error (MSE), Reduction of Error (RE), and Coefficient of Efficiency (CE) Statistics Calculated Over the Calibration and Verification Periods Between the $T\delta^{18}O_{shell}$ Series Generated Using Both the Royer et al. (2013) and Grossman and Ku (1986) Palaeotemperature Equations*

| | Arithmetic mean summer | | | | | Arithmetic mean growing season | | | | | Weighted mean growing season | | | | |
|---|---|---|---|---|---|---|---|---|---|---|---|---|---|---|---|
| | $R$ | $R^2$ | MSE | | | $R$ | $R^2$ | MSE | | | $R$ | $R^2$ | MSE | | |
| | | | | | | *Grossman and Ku (1986)* | | | | | | | | | |
| Constant salinity | | | | | | | | | | | | | | | |
| Calibration | 0.70 | 0.49 | 0.47 | RE | 0.32 | 0.72 | 0.52 | 0.42 | RE | 0.26 | 0.67 | 0.45 | 0.42 | RE | 0.20 |
| Verification | 0.61 | 0.37 | 0.42 | CE | 0.31 | 0.57 | 0.33 | 0.79 | CE | −0.96 | 0.60 | 0.36 | 0.26 | CE | 0.35 |
| Variable salinity | | | | | | | | | | | | | | | |
| Calibration | 0.68 | 0.47 | 0.53 | RE | 0.23 | 0.71 | 0.50 | 0.40 | RE | 0.28 | 0.65 | 0.42 | 0.47 | RE | 0.10 |
| Verification | 0.54 | 0.29 | 0.48 | CE | 0.21 | 0.50 | 0.25 | 0.93 | CE | −1.29 | 0.50 | 0.25 | 0.32 | CE | 0.39 |
| | | | | | | *Royer et al. (2013)* | | | | | | | | | |
| Constant salinity | | | | | | | | | | | | | | | |
| Calibration | 0.70 | 0.49 | 0.41 | RE | 0.40 | 0.68 | 0.47 | 0.41 | RE | 0.26 | 0.64 | 0.41 | 0.33 | RE | 0.32 |
| Verification | 0.61 | 0.37 | 1.03 | CE | −0.69 | 0.60 | 0.36 | 0.91 | CE | −1.16 | 0.59 | 0.35 | 0.67 | CE | −0.77 |
| Variable salinity | | | | | | | | | | | | | | | |
| Calibration | 0.68 | 0.47 | 0.41 | RE | 0.41 | 0.66 | 0.44 | 0.40 | RE | 0.28 | 0.63 | 0.39 | 0.33 | RE | 0.33 |
| Verification | 0.54 | 0.29 | 1.11 | CE | −0.83 | 0.51 | 0.26 | 1.00 | CE | −1.37 | 0.48 | 0.23 | 0.75 | CE | −0.98 |

*Note*. The data were calibrated over the time interval from 1980 to 2007 and verified using the independent instrumental data over the period 1954–1979. The $T\delta^{18}O_{shell}$ data were calibrated against arithmetic mean summer (June–August) and arithmetic and weighted mean growing season SWTs in the Keppel pier instrumental record. The reconstruction is deemed robust if the RE and CE statistics are >0.

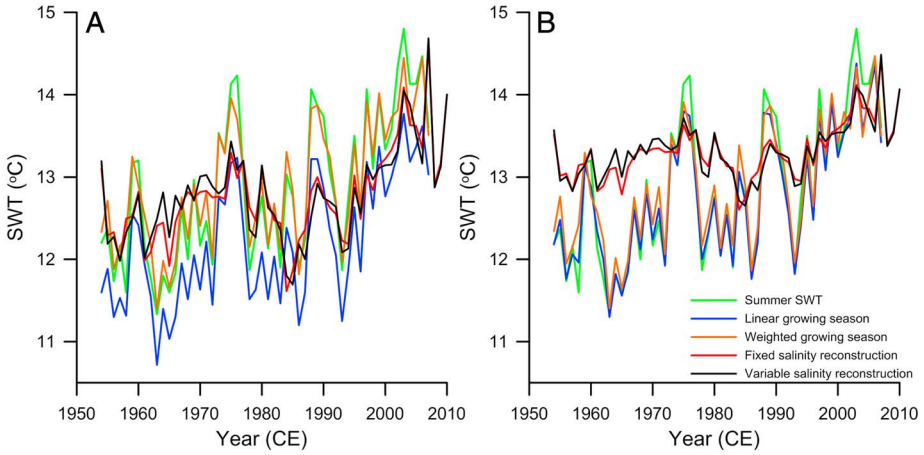


**Figure 8.** Comparison of the $T\delta^{18}O_{shell}$ series derived using (a) the Grossman and Ku (1986) and (b) the Royer et al. (2013) palaeotemperature equations using both variable and constant salinity approaches (black and red lines, respectively). The green lines show arithmetic mean summer (June to August) SWTs, while the blue and orange lines show the arithmetic and weighted mean growing season SWTs, respectively.

($R = 0.38$, $P = 0.14$, calculated over the period 1958–2010). Multiple linear regression model analyses indicated that biological productivity (phytoplankton and zooplankton abundance) and SWT variability can explain 68% ($F = 4.02$, $P < 0.001$) of the variability in the *G. glycymeris* growth increment width chronology. The multiple linear regression model indicated that biological productivity alone (excluding SWT variability) can explain 48% ($F = 2.74$, $P < 0.05$) of the variability in the *G. glycymeris* growth increment width chronology. The multiple linear regression model indicates that primary productivity can explain 39% ($F = 2.09$, $P < 0.05$) of the variability in the *G. glycymeris* growth increment width chronology.

## 5. Discussion

### 5.1. Subannual Analyses

The subannual sequential sampling strategy, which generated continuous carbonate samples throughout a series of growth increments from eight independent shells, provides data that facilitate the assessment of the seasonal timing of shell growth and the formation of the growth line. Previous assessments, which assumed a linear subannual growth rate, have suggested that the growth check (line) forms during the winter months with growth predominantly occurring during the spring and summer months (Royer et al., 2013). Although there were differences in the duration of the suggested growing season between the subannually resolved $T\delta^{18}O_{shell}$ data derived using the Grossman and Ku (1986) and Royer et al. (2013) equations (May–October and June–September, respectively) both approaches indicate that the growth check in the *G. glycymeris* population in the Tiree Passage likely starts to form shortly after peak SWTs are reached in autumn with little, if any, growth occurring over the winter months. While the subannual $T\delta^{18}O_{shell}$ data do not incorporate any reconstructed SWTs that would be characteristic of winter SWTs, these data do not unequivocally indicate that the *G. glycymeris* shells do not grow during the winter months. As has been shown in some *A. islandica* populations, it could be the case that *G. glycymeris* continues to grow at a greatly reduced rate over the winter months (Schöne, 2013). However, the reduced growth rate over the winter interval must be sufficiently slow that the winter growth makes up a relatively small percentage of the 150 μm sampling resolution used for the subannual analyses. As such the remaining portion of the sample, which would have

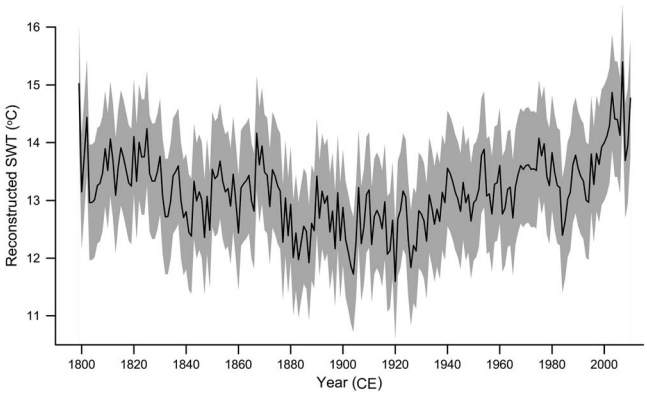


**Figure 9.** Reconstructed SWTs ($T\delta^{18}O_{shell}$) over the time interval 1799–2010 (black line). The shaded gray area represents a 1$\sigma$ error envelope corresponding to the sum of the salinity uncertainty, intershell $\delta^{18}O_{shell}$ variability and external precision. Calibration equation MSE = ±0.3°C, external precision = ±0.2°C, and mean intershell variability = ±0.6°C.

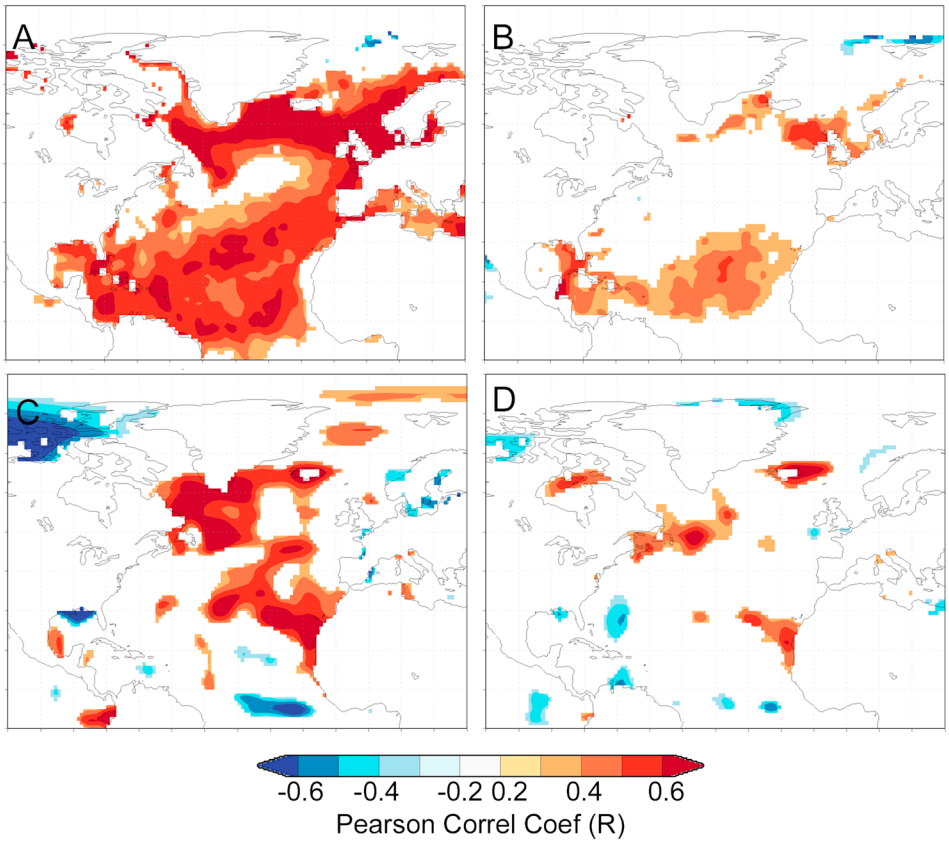


**Figure 10.** Spatial correlation analyses between the annually resolved T$\delta^{18}O_{shell}$ record and (a) raw and (b) linear detrended mean May to October HadISST1 gridded sea surface temperatures; and (c) raw and (d) linear detrended mean May to October EN4 SSS gridded sea surface salinity; correlations calculated over the calibration period from 1980 to 2007. All correlations shown are significant at $P < 0.1$. Correlations calculated using KNMI Climate Explorer Facility (Trouet & Van Oldenborgh, 2013).

formed as growth rates increase during spring, would mask any winter signal, thus leading to the first sample containing a reconstructed SWT corresponding to spring water temperatures. However, while developing a more detailed understanding of the absolute timing of the *G. glycymeris* growing season in the Tiree Passage is an important future objective, the priority with the current analyses is to determine the likely seasonal bias of the annually resolved $\delta^{18}O_{shell}$ data. The coherence between the subannually resolved T$\delta^{18}O_{shell}$ series with the Tiree Passage, Keppel Pier, and HadISST1 SST data sets from northwest Scotland (Figures 6 and 7) strongly indicates that the peak growing season of the Tiree Passage *G. glycymeris* population is likely from late spring through to late summer, which is in agreement with other *G. glycymeris* populations (Royer et al., 2013). As with other marine bivalves, however, it is likely that the precise seasonality of growth is associated with local environmental conditions, and thus, the growing season may differ across study localities with different environmental settings.

The suggested duration of the *G. glycymeris* growing season (approximately 6 and 4 months using the Grossman & Ku, 1986, and the Royer et al., 2013, palaeotemperature equations, respectively) and maximum subannual sampling resolutions (22 samples per increment) suggests that it is possible to reconstruct up to subweekly resolution SWT variability in the Tiree Passage. The mean subannual sampling resolution (13.7 samples per increment) corresponds to approximately fortnightly resolution.

### 5.2. Subannual Growth Rate Assessment

Despite the high-temporal resolution of the subannually resolved T$\delta^{18}O_{shell}$ data the fact that the instrumental observations from this region are only available at monthly resolution limits our ability to provide a thorough assessment of the suggestion that the rate of subannual *G. glycymeris* shell growth is constant throughout the growing season. However, the application of both arithmetic and weighted mean growing

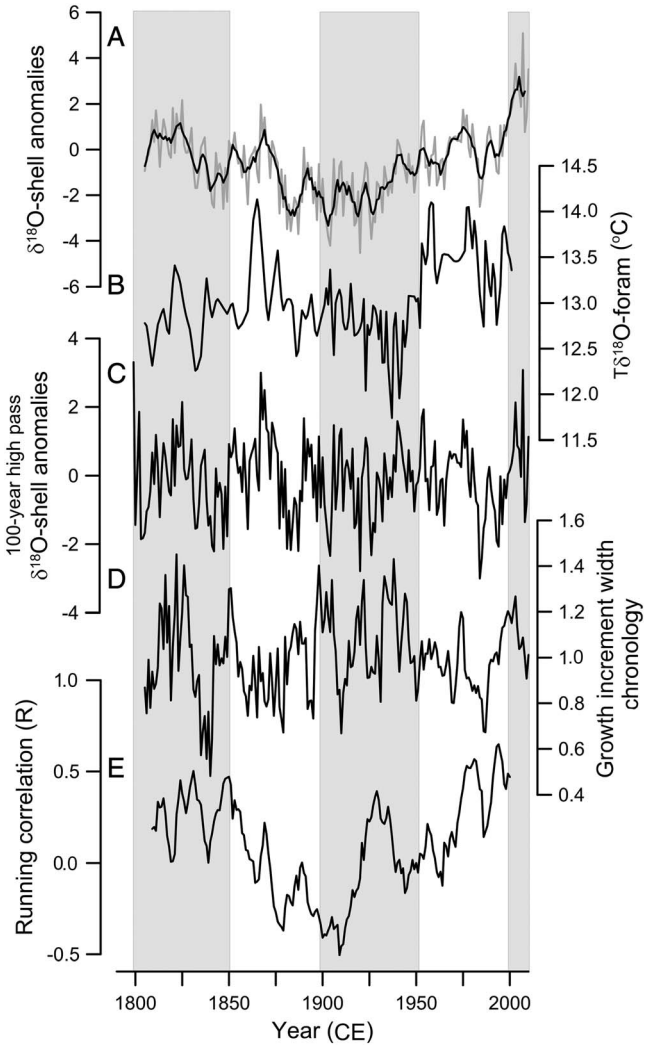


**Figure 11.** Comparison between (a) the $\delta^{18}O_{shell}$ data; (b) reconstructed SWTs from the Loch Sunart $T\delta^{18}O$-foram record (Cage & Austin, 2010); (c) 100 year high-pass filtered $\delta^{18}O_{shell}$ data; (d) the *G. glycymeris* ARSTAN growth increment width chronology index (Reynolds et al., 2013). (e) Twenty year running correlations calculated between the 100 year high-pass filtered $\delta^{18}O_{shell}$ data and the growth increment width chronology index.

season SWT series as target environmental parameters provided an opportunity to evaluate the likelihood of whether *G. glycymeris* subannual shell growth forms at a constant rate throughout the growing season. In theory, if the shell forms at constant rate throughout the growing season then the annually resolved $T\delta^{18}O_{shell}$ reconstruction should perform best against the arithmetic mean growing season SWT target parameter as each month used to compute the mean SWT is equally weighted. Our analyses, however, indicate that using both the Grossman and Ku (1986) and the Royer et al. (2013) equations, the $T\delta^{18}O_{shell}$ reconstructions perform better against the weighted mean growing season SWTs than against the arithmetic mean growing season SWTs (Table 1). Given the weighting function applied was Gaussian corresponding to a peak weighting during August to September and reduced weighting at the onset and end of the growing season (see supporting information), these results strongly support the suggestion that *G. glycymeris* seasonal growth is not constant. These results and the frequency distribution of the subannually resolved $T\delta^{18}O_{shell}$ data (Figure 6), which show a predominant bias toward the summer SWTs, suggest that the subannual shell growth of *G. glycymeris* in the Tiree Passage is likely to be greatest during the summer with slower rates of growth in early spring and at the end of the peak growing season (autumn).

### 5.3. Thermal Threshold of Growth

It has previously been proposed that *G. glycymeris* has a minimum thermal threshold for growth of 12.9°C (Royer et al., 2013), which could limit the application of *G. glycymeris* records for reconstructing SWTs through intervals characterized by colder climate conditions, such as the so-called Little Ice Age (ca. 1450–1850), or in more northerly, cooler, regions of the North Atlantic. Our data, however, suggest reconstructed SWTs in the subannual $T\delta^{18}O_{shell}$ series extend down to minimum values of 8.8°C and 9.3°C, using the Grossman and Ku (1986) and the Royer et al. (2013) equations, respectively. These data therefore indicate that *G. glycymeris* shell growth does occur in SWT's below the suggested 12.9°C growth threshold. Nonetheless, with these currently available data we are not able to firmly rule out the possibility that a thermal threshold on growth does exist in *G. glycymeris*, and a much broader study incorporating samples from a wider spectrum of environments would be required to test this hypothesis.

### 5.4. Reconstruction Calibration

While it was not the primary scope of this paper to conduct an assessment of Grossman and Ku (1986) and the Royer et al. (2013) palaeotemperature equations, comparison of the subannual and annually resolved $T\delta^{18}O_{shell}$ series converted using each equation does provide scope for a preliminary assessment of the validity of both calibrations in reconstructing past SWT variability. The comparison between the annually resolved $T\delta^{18}O_{shell}$ series against the three target SWT series (arithmetic mean summer and arithmetic and weighted mean growing season, with independent growing seasons applied to the Grossman & Ku, 1986, and Royer et al., 2013, derived reconstructions) highlighted that the $T\delta^{18}O_{shell}$ series can explain a significant proportion of observed SWT variability of the instrumental time interval (Table 1). Over the calibration period both palaeotemperature equations resulted in $T\delta^{18}O_{shell}$ data that contained significant skill at reconstructing SWT variability over the calibration period (1980–2007; RE $>$ 0; Table 1). However, only the $T\delta^{18}O_{shell}$ data derived using the Grossman and Ku (1986) equation contained significant skill over both the calibration and verification periods (RE and CE $>$ 0; Table 1). The $T\delta^{18}O_{shell}$ data derived using the Royer et al. (2013) equation over the verification period were on average 0.7 ± 0.06°C too warm across the three target

parameters. The differences between the reconstructed SWT data using the Grossman and Ku (1986) and Royer et al. (2013) equations are due to differences in the gradients (sensitivity) of the empirically derived equations, with the Grossman and Ku (1986) equation generating a reconstruction with a higher amplitude of variability due to its greater sensitivity.

Royer et al. (2013) derived the *G. glycymeris* species-specific palaeotemperature equation to account for an offset in their reconstructed SWTs, derived using the Grossman and Ku (1986) equation, from the instrumental SWTs at their sampling site. In their study Royer et al. (2013) assumed that *G. glycymeris* had a constant rate of growth during the growing season. Our data, however, suggest that such an assumption is likely incorrect. The difference in skill of the $T\delta^{18}O_{shell}$ reconstructions using the Grossman and Ku (1986) equation when compared to arithmetic mean growing season and weighted growing season reconstructions suggests that the failure to take into account a nonlinear growth rate over the growing season could account for a significant proportion of the offset between the reconstructed SWTs. For instance, the $T\delta^{18}O_{shell}$ data, generated using the Grossman and Ku (1986) equation when calibrated against weighted mean growing season SWTs, contain significant RE and CE statistics (RE and CE $>$ 0; Table 1). However, the Grossman and Ku (1986) derived $T\delta^{18}O_{shell}$ data reconstruction of arithmetic mean growing season SWTs contain a mean offset from the instrumental data of +0.7°C, comparable to the offset we find when using the Royer et al. (2013) equation. In addition, the $T\delta^{18}O_{shell}$ reconstruction of arithmetic mean growing season SWTs has a nonsignificant CE statistic and a MSE over the verification period more than two to three times that of the weighted mean SWT reconstruction (MSE = 0.79°C and 0.98°C compared to 0.26°C and 0.32°C, respectively; Table 1). While the application of the two palaeotemperature equations does not change the overall patterns of variability contained in the raw $\delta^{18}O_{shell}$ data, the equations do generate differences in the quantitative reconstruction of absolute SWTs. It is therefore clear from these analyses that future studies need to adopt approaches to evaluate the nature of subannual growth rates to accurately derive the seasonal bias captured by the annually resolved $\delta^{18}O_{shell}$ series.

### 5.5. Salinity/$\delta^{18}O_w$ Uncertainty

Given the lack of observational $\delta^{18}O_w$ data, required for reconstructing past SWT variability from $\delta^{18}O_{shell}$ records, the effects of varying salinity and therefore $\delta^{18}O_w$ data were evaluated over the instrumental period. The comparison between the $T\delta^{18}O_{shell}$ series derived using constant and variable salinity values over the instrumental period, as well as examining the calibration verification statistics, provided two ways of assessing the $\delta^{18}O_w$ uncertainties. The low MSE (0.02°C) calculated between the $T\delta^{18}O_{shell}$ series derived using the Grossman and Ku (1986) equation using both the constant and variable salinity approaches over the calibration period suggests that uncertainties associated with salinity variability are negligible in our $T\delta^{18}O_{shell}$ series. The significant RE and CE statistics (Table 1) for the $T\delta^{18}O_{shell}$ reconstructions, derived using both the constant and variable salinity values, and the negligible difference in reconstructed SWTs calculated using the two salinity approaches, indicates that variability in the $\delta^{18}O_{shell}$ record is dominated by SWT variability with SSS playing only a negligible role. We argue therefore that using a constant salinity-based approach to convert $\delta^{18}O_{shell}$ record into absolute SWTs in the Tiree Passage can produce a robust and skillful SWT reconstruction over, at least, the past two centuries. Using the modern salinity range between ~33.5 and 35 across the Hebridean shelf (Inall et al., 2009) suggests a corresponding SWT uncertainty of ±0.59°C.

### 5.6. Broad-Scale Variability

Physical and geochemical variability across the Sea of the Hebrides is closely coupled to that of the wider North Atlantic with variations in local currents (e.g., ESC) reflecting variations in local wind stress, SPG dynamics, and broader changes in the AMOC (Holliday et al., 2015; Huthnance et al., 2009; Inall et al., 2009; Marsh et al., 2017; Xu et al., 2015). The examination of the sensitivity of the $T\delta^{18}O_{shell}$ series against North Atlantic SWTs and SSSs indicates that the variability contained in the Tiree Passage *G. glycymeris* shells reflect the connectivity of the local hydrographic setting to the wider North Atlantic system (Figure 10). The spatial pattern of the correlations between the $T\delta^{18}O_{shell}$ series and North Atlantic SWTs broadly coincides with the eastern boundary currents of the SPG system suggesting that the variability contained in the $T\delta^{18}O_{shell}$ series is reflecting SWT variability across the Sea of the Hebrides and the adjacent northeast Atlantic waters.

Intriguingly, while no significant correlations were identified between the $T\delta^{18}O_{shell}$ series and local salinity variability, highly significant correlations were identified between the $T\delta^{18}O_{shell}$ series and SSS variability

over the western region of the SPG and in the Labrador Sea (Figure 10). The Labrador Sea is a key area of deepwater formation, contributing around one third toward the deep limb of the AMOC, and drives changes in the North Atlantic surface hydrography, mainly the SPG circulation (e.g., Rhein et al., 2002; Talley, 2003). The positive correlations identified between the $T\delta^{18}O_{shell}$ series and SSS variability over the broader Labrador Sea region suggest that periods characterized by high (low) salinity (and presumably density) here coincide with periods of warm (cold) conditions in the Northeast Atlantic and the Sea of the Hebrides. Given that increases (decreases) in seawater density across the Labrador Sea region are associated with an increases (decreases) in the production of Labrador Sea Water (LSW; Marshall & Schott, 1999), this pattern of correlations would implicate that a proportion of the variability contained in the $T\delta^{18}O_{shell}$ series likely reflects the local SWT variability that is brought about by changes in SPG circulation pattern of the North Atlantic associated with the LSW formation. This interpretation is supported by the pattern of the spatial correlations between the $T\delta^{18}O_{shell}$ series and North Atlantic SWTs with the correlations broadly following the distribution of the surface boundary currents of the SPG across the Northeast Atlantic region. It should be noted, however, that given the coastal locality of the $T\delta^{18}O_{shell}$ series the variability captured in the reconstruction clearly reflects a proportion of local-scale variability coupled with that of the broader North Atlantic region. Thus, it would be inappropriate to interpret the single $T\delta^{18}O_{shell}$ series as a direct reconstruction of changes in North Atlantic circulation dynamics.

### 5.7. Multiproxy Analyses

The availability of three independent proxy records from the Tiree Passage and adjacent Loch Sunart (the new $T\delta^{18}O_{shell}$ series presented here, the *G. glycymeris* growth increment width chronology (Reynolds et al., 2013), and the Loch Sunart benthic foraminifera $\delta^{18}O$ record, Cage & Austin, 2010; Figure 11) provides the opportunity for a more detailed analysis of the past environmental variability in this region. However, while the three records have each been robustly and independently calibrated to reconstruct past SWT variability, which should suggest an element of coherence between the records, the comparison of the three records is complicated by subtle differences in seasonality, temporal resolution, and the frequency domains captured by each reconstruction. For example, the $T\delta^{18}O_{shell}$ series and the *G. glycymeris* growth increment width chronology, which were built from the same *G. glycymeris* shell material, capture different frequency domains. The growth increment width chronology contains only the high-frequency component of variability due to the application of detrending techniques during the construction of the chronology (Reynolds et al., 2013). Given that no detrending techniques were applied to the $T\delta^{18}O_{shell}$ series, the variability it contains should more closely reflect that of the environment. Furthermore, as the low-frequency variability contained in the growth increment width chronology is a function of the mean segment length, related to the mean longevity of the shells contained in the chronology, which is variable through time, portions of the chronology that contain shells with greater (lower) mean longevities contain a higher (lower) degree of low-frequency variability (Cook et al., 1995). In contrast, the benthic foraminifera $\delta^{18}O$ record, which is generated by the analysis of a sediment core, is relatively deficient in the high-frequency domain, due to the relatively lower temporal sampling resolution, and therefore captures a greater proportion of the low-frequency variability.

Despite these potential complications, the $T\delta^{18}O_{shell}$ and the Loch Sunart benthic $\delta^{18}O$ series (Cage & Austin, 2010) show significant, albeit weak, coherence over the last two centuries ($R = 0.23$, $P < 0.05$, 1799–2001). Differences between the $T\delta^{18}O_{shell}$ series and SWTs reconstructed from the benthic $\delta^{18}O$ series could be due to a multitude of factors such as environmental differences between Loch Sunart main basin and the Tiree Passage, varying sedimentation rates and/or variable seasonality in the benthic $\delta^{18}O$ record due to foraminiferal migration within the water column. Due to the age uncertainties in the benthic $\delta^{18}O$ record the generation of a longer-term $T\delta^{18}O_{shell}$ series from the Tiree Passage is required to provide a more robust evaluation of the mechanisms behind the differences in the two records.

While significant correlations were identified between the $T\delta^{18}O_{shell}$ series and the *G. glycymeris* growth increment width chronology over some time intervals, for example, from 1950 to 2010, the relationship is highly variable (Figure 11). The variable coherence between the two series provides insights into the possible drivers of the variability in both the proxy archives and in the Tiree Passage.

Hitherto, the biological mechanism that drives the growth increment variability in *G. glycymeris* is not known. The examination of the relationships between the *G. glycymeris* chronology and SST variability,

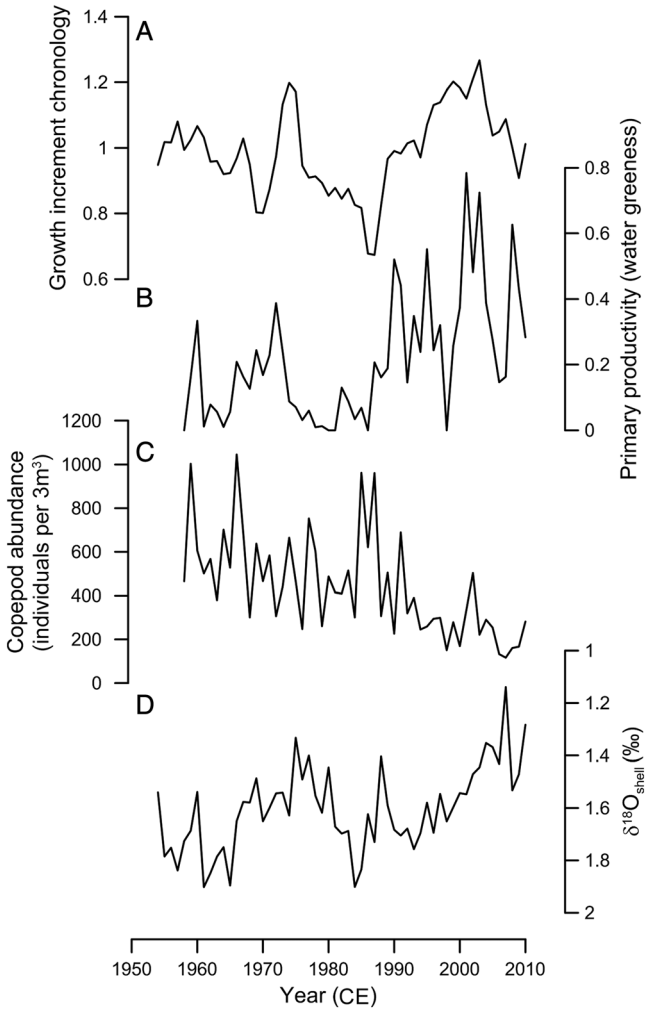


**Figure 12.** Comparison between the AR *G. glycymeris* growth increment width chronology and biological productivity on the Hebridean shelf. (a) The annually resolved *G. glycymeris* growth increment width sclerochronology (Reynolds et al., 2013). (b) Level of primary productivity measured by the greenness of samples. (c) Copepod abundance. (d) The annually resolved $\delta^{18}O_{shell}$ series. Primary productivity and copepod abundance recorded across the 55–60°N by 0–10°W grid box from the Continuous Plankton Recorder (CPR) survey data set (https://www.sahfos.ac.uk/DOI:10.7487/2017.216.1.1072).

phytoplankton abundance, and zooplankton abundance on the Hebridean shelf provides the opportunity to evaluate the biological mechanisms that drive *G. glycymeris* shell growth and reconcile the differences between the chronology and the T$\delta^{18}O_{shell}$ series. Although the growth increment widths have been shown to be sensitive to SWT variability (Brocas et al., 2013; Reynolds et al., 2013) it is likely that SWT is a secondary driver of growth, with the growth increments primarily driven by primary productivity dynamics (quantity and nutritious value of the food supply) which are in turn related to SWT, as has been demonstrated in other temperate marine bivalves such as *A. islandica* (Wanamaker et al., 2009; Witbaard et al., 2003). The significant, albeit relatively weak, relationship between the *G. glycymeris* and the phytoplankton abundance indicates that primary productivity likely plays a significant role in driving *G. glycymeris* shell growth in the Tiree Passage. However, the results of the multiple linear regression model analyses and linear regression analyses indicate that primary productivity is unlikely to be the sole biological mechanism that influences *G. glycymeris* shell growth. For instance, the multiple linear regression model incorporating total biological productivity (zooplankton and phytoplankton abundance) can explain 48% ($P < 0.05$) of the variability in *G. glycymeris* shell growth compared to 38% ($P < 0.05$) that could be explained by primary productivity alone. The stronger relationship of the growth increment chronology with biological productivity is likely due to the model incorporating the reduction in food quality and/or quantity associated with an increase in zooplankton abundance leading to an overall negative impact on shell growth. Similar relationships have been reported between *A. islandica* populations and zooplankton abundance in the North Sea (Witbaard et al., 2003). Visually examining the relationship between primary productivity, zooplankton abundance, and the *G. glycymeris* chronology highlights this pattern (Figure 12). For instance, over the interval 1980–1990 primary productivity is at a relatively low level, albeit with a slight increasing trend. Over this interval zooplankton abundance (copepods) exhibits a pronounced spike. The enhanced level of competition for the relatively low level of food during this period leads to the *G. glycymeris* shells having their worst period of shell growth recorded over the instrumental period. The likely mechanism linking zooplankton abundance and *G. glycymeris* shell growth is that the zooplankton reduce the abundance of high-quality food from the water column and lead to an increase in the level of low-quality food sources (fecal matter). The negative correlation between zooplankton and *G. glycymeris* shell growth indicates that the reduced food quality combined with the reduced level of higher-quality food is the likely biological mechanism driving *G. glycymeris* shell growth. The fact that the multiple linear regression model combining biological productivity and SST variability improves the correlation over both the biological productivity and primary productivity models (68% compared to 48% and 38%, respectively) indicates that SWT variability is likely still a dominant mechanism in driving *G. glycymeris* shell growth.

Given the relationship between the *G. glycymeris* growth increment width chronology and biological productivity and SSTs, differences between the variability in the *G. glycymeris* growth increment width chronology and the T$\delta^{18}O_{shell}$ series could therefore be driven by several mechanisms. First, we discount the possibility that these differences are associated to ontogenetic (age related) shifts in the seasonality of *G. glycymeris* shell growth. The fact that shells of different ontogenetic ages have been successfully cross-dated (Brocas et al., 2013; Reynolds et al., 2013) and the $\delta^{18}O_{shell}$ data, derived from increments of different ontogenetic ages, contain coherent variability suggests that the *G. glycymeris* has a constant growing season throughout the lifetime of each specimen. Given primary productivity is greatest at the sea surface, associated with SST

variability (Richardson & Schoeman, 2004), SSS variability (Mollmann et al., 2003), and circulation patterns (Reid et al., 2003), and the $\delta^{18}O$ variability contained in the *G. glycymeris* shells corresponds to that of the ambient water surrounding the shell on the seabed (~24–55 m water depth); differences in the relationship between the growth increment width chronology and $\delta^{18}O_{shell}$ derived proxies are likely related to differences between seafloor and sea surface environmental conditions and/or changes in biological productivity.

## 6. Conclusions

In this study we demonstrate that subannual and annually resolved $\delta^{18}O$ analyses derived from the growth increments of the long-lived marine bivalve *G. glycymeris* can reconstruct past summer SWTs on subannual to multicentennial time scales. The resulting reconstruction, which passes statistical tests of significance and skill, can therefore be used to quantify the amplitude and frequency of past SWT variability that will ultimately lead to the development of a better understanding of the mechanisms and drivers of the coupled ocean-atmosphere system. Analyses of the reconstructed SWTs with the *G. glycymeris* growth increment width chronology and records of biological productivity highlight that *G. glycymeris* shell growth is likely driven by the combined influence of SST variability and the abundance and quality of food supply. The availability of fossil *G. glycymeris* shell material from western Scotland dating back to at least the early Holocene and the apparent sensitivity of the reconstruction to broad-scale variability across the Northeast Atlantic region indicates that these methods could facilitate the reconstruction of past marine variability, at seasonal to millennial time scales, spanning the entire Holocene period.

**Acknowledgments**
We thank the Captain and crew of the RV *Prince Madog* and the members of the NERC Facility for Scientific Diving (NFSD) for the collection of the shell material. This work was supported by the NERC-funded CLAM project; (project NE/N001176/1). We thank Alexandra Nederbragt (Cardiff University) for providing technical support. We would like to thank the three anonymous reviewers for their helpful comments in reviewing this manuscript. These stable isotope data presented in this study are available at https://www.ncdc.noaa.gov/paleo/study/22621.

## References

Berthou, P., Blanchard, M., Noel, P., & Vergnaud-Grazzini, C. (1986). The analysis of stable isotopes of the shell applied to the determination of the age of four bivalves of the "Normano-Breton" Gulf, Western Channel. *ICES, K*, *16*, 1–13.

Black, B. A. (2009). Climate-driven synchrony across tree, bivalve, and rockfish growth-increment chronologies of the northeast Pacific. *Marine Ecology Progress Series*, *378*, 37–46.

Black, B. A., Sydeman, W. J., Frank, D. C., Griffin, D., Stahle, D. W., Garcia-Reyes, M., … Peterson, W. T. (2014). Climate change. Six centuries of variability and extremes in a coupled marine-terrestrial ecosystem. *Sciences*, *345*(6203), 1498–1502. https://doi.org/10.1126/science.1253209

Brocas, W. M., Reynolds, D. J., Butler, P. G., Richardson, C. A., Scourse, J. D., Ridgway, I. D., & Ramsay, K. (2013). The dog cockle, *Glycymeris glycymeris* (L.), a new annually-resolved sclerochronological archive for the Irish Sea. *Palaeogeography, Palaeoclimatology, Palaeoecology*, *373*, 133–140.

Broecker, W. S. (1998). Paleocean circulation during the last deglaciation: A bipolar seesaw? *Paleoceanography*, *13*(2), 119–121. https://doi.org/10.1029/97PA03707

Butler, P. G., Richardson, C. A., Scourse, J. D., Wanamaker, A. D., Shammon, T. M., & Bennell, J. D. (2010). Marine climate in the Irish Sea: Analysis of a 489-year marine master chronology derived from growth increments in the shell of the clam *Arctica islandica*. *Quaternary Science Reviews*, *29*(13–14), 1614–1632. https://doi.org/10.1016/j.quascirev.2009.07.010

Butler, P. G., Wanamaker, A. D., Scourse, J. D., Richardson, C. A., & Reynolds, D. J. (2013). Variability of marine climate on the North Icelandic Shelf in a 1357-year proxy archive based on growth increments in the bivalve *Arctica islandica*. *Palaeogeography, Palaeoclimatology, Palaeoecology*, *373*, 141–151. https://doi.org/10.1016/j.palaeo.2012.01.016

Cage, A. G., & Austin, W. E. N. (2010). Marine climate variability during the last millennium: The Loch Sunart record, Scotland, UK. *Quaternary Science Reviews*, *29*(13-14), 1633–1647.

Cook, E. R., Briffa, K. R., Meko Graybill, D. M. D. A., & Funkhouser, G. (1995). The "segment length curse" in long tree-ring chronology development for palaeoclimatic studies. *The Holocene*, *5*(2), 229–237. https://doi.org/10.1177/095968369500500211

Ebisuzaki, W. (1997). A method to estimate the statistical significance of a correlation when the data are serially correlated. *Journal of Climate*, *10*(9), 2147–2153.

Good, S. A., Martin, M. J., & Rayner, N. A. (2013). EN4: Quality controlled ocean temperature and salinity profiles and monthly objective analyses with uncertainty estimates. *Journal of Geophysical Research: Oceans*, *118*, 6704–6716. https://doi.org/10.1002/2013JC009067

Grossman, E., & Ku, T. (1986). Oxygen and carbon isotope fractionation in biogenic aragonite: Temperature effects. *Chemical Geology*, *59*, 59–74. https://doi.org/10.1016/0168-9622(86)90057-6

Halfar, J., Hetzinger, S., Adey, W., Zack, T., Gamboa, G., Kunz, B., … Jacob, D. E. (2011). Coralline algal growth-increment widths archive North Atlantic climate variability. *Palaeogeography, Palaeoclimatology, Palaeoecology*, *302*(1-2), 71–80.

Hall, I. R., Boessenkool, K. P., Barker, S., Mccave, I. N., & Elderfield, H. (2010). Surface and deep ocean coupling in the subpolar north atlantic during the last 230 years. *Paleoceanography*, *25*, PA2101. https://doi.org/10.1029/2009PA001886

Hayward, P. J., & Ryland, J. S. (1995). *Handbook of the marine fauna of North-West Europe*. Oxford: Oxford University Press.

Helama, S., Schöne, B. R., Kirchhefer, A. J., Nielsen, J. K., Rodland, D. L., & Janssen, R. (2007). Compound response of marine and terrestrial ecosystems to varying climate: Pre-anthropogenic perspective from bivalve shell growth increments and tree-rings. *Marine Environmental Research*, *63*(3), 185–199.

Holliday, N. P., Cunningham, S. A., Johnson, C., Gary, S. F., Griffiths, C., Read, J. F., & Sherwin, T. (2015). Multidecadal variability of potential temperature, salinity, and transport in the eastern subpolar North Atlantic. *Journal of Geophysical Research: Oceans*, *120*, 5945–5967. https://doi.org/10.1002/2015JC010762

Holt, J., Butenschon, M., Wakelin, S. L., Artioli, Y., & Allen, J. I. (2012). Oceanic controls on the primary production of the northwest European continental shelf: Model experiments under recent past conditions and a potential future scenario. *Biogeosciences*, *9*(1), 97–117.

Hudson, J. H., Shinn, E. A., Halley, R. B., & Lidz, B. (1976). Sclerochronology: A tool for interpreting past environments. *Geology*, *4*(6), 361. https://doi.org/10.1130/0091-7613(1976)4%3C361:SATFIP%3E2.0.CO;2

Hurrell, J. W., & Trenberth, K. E. (1999). Global sea surface temperature and analyses: Multiple problems and their implications for climate analysis, modeling, and reanalysis. *Bulletin of the American Meteorological Society*, *80*(12), 2661–2678. https://doi.org/10.1175/1520-0477(1999)080%3C2661:GSSTAM%3E2.0.CO;2

Hut, G. (1987). *Consultants group meeting on stable isotope reference samples for geochemical and hydrological investigations* (p. 42). Vienna: International Atomic Energy Agency.

Huthnance, J. M., Holt, J. T., & Wakelin, S. L. (2009). Deep ocean exchange with west-European shelf seas. *Ocean Science*, *5*(4), 621–634.

Inall, M., Gillibrand, P., Griffiths, C., MacDougal, N., & Blackwell, K. (2009). On the oceanographic variability of the North-West European Shelf to the West of Scotland. *Journal of Marine Systems*, *77*(3), 210–226.

Jones, D. S. (1980). Annual cycle of shell growth increment formation in 2 continental-shelf bivalves and its paleoecologic significance. *Paleobiology*, *6*(03), 331–340. https://doi.org/10.1017/S0094837300006837

Jones, D. S., Arthur, M. A., & Allard, D. J. (1989). Sclerochronological records of temperature and growth from shells of *Mercenaria mercenaria* from Narragansett Bay, Rhode Island. *Marine Biology*, *102*(2), 225–234. https://doi.org/10.1007/BF00428284

Kamenos, N. A. (2010). North atlantic summers have warmed more than winters since 1353, and the response of marine zooplankton. *Proceedings of the National Academy of Sciences of the United States of America*, *107*(52), 22,442–22,447.

Kim, S. T., Mucci, A., & Taylor, B. E. (2007). Phosphoric acid fractionation factors for calcite and aragonite between 25 and 75°C: Revisited. *Chemical Geology*, *246*(3-4), 135–146.

Lohmann, G., & Schöne, B. R. (2013). Climate signatures on decadal to interdecadal time scales as obtained from mollusk shells (*Aarctica islandica*) from Iceland. *Palaeogeography Palaeoclimatology Palaeoecology*, *373*, 152–162.

Lund, D. C., Lynch-Stieglitz, J., & Curry, W. B. (2006). Gulf stream density structure and transport during the past millennium. *Nature*, *444*, 601–604.

Marchitto, T. M., Jones, G. A., Goodfriend, G. A., & Weidman, C. R. (2000). Precise temporal correlation of Holocene mollusk shells using sclerochronology. *Quaternary Research*, *53*(02), 236–246.

Marsh, R., Haigh, I. D., Cunningham, S. A., Inall, M. E., Porter, M., & Moat, B. I. (2017). Large-scale forcing of the european slope current and associated inflows to the north sea. *Ocean Science*, *13*, 315–335.

Marshall, J., & Schott, F. (1999). Open-ocean convection: Observations, theory, and models. *Reviews of Geophysics*, *37*(1), 1–64.

Mette, M. J., Wanamaker, A. D. Jr., Carroll, M. L., Ambrose, W. G. Jr., & Retelle, M. J. (2016). Linking large-scale climate variability with *Arctica islandica* shell growth and geochemistry in northern Norway. *Limnology and Oceanography*, *61*(2), 748–764. https://doi.org/10.1002/lno.10252

Mjell, T. L., Ninnemann, U. S., Kleiven, H. F., & Hall, I. R. (2016). Multidecadal changes in iceland scotland overflow water vigor over the last 600 years and its relationship to climate. *Geophysical Research Letters*, *43*, 2111–2117. https://doi.org/10.1002/2016GL068227

Moffa-Sánchez, P., Born, A., Hall, I. R., Thornalley, D. J. R., & Barker, S. (2014). Solar forcing of north atlantic surface temperature and salinity over the past millennium. *Nature Geoscience*, *7*, 275–278.

Moffa-Sánchez, P., Hall, I. R., Barker, S., Thornalley, D. J. R., & Yashayaev, I. (2014). Surface changes in the eastern labrador sea around the onset of the little ice age. *Paleoceanography*, *29*, 160–175. https://doi.org/10.1002/2013PA002523

Mollmann, C., Kornilovs, G., Fetter, M., Koster, F. W., & Hinrichsen, H. H. (2003). The marine copepod, *Pseudocalanus elongatus*, as a mediator between climate variability and fisheries in the Central Baltic Sea. *Fisheries Oceanography*, *12*(4-5), 360–368.

North, G. R., Biondi, F., Bloomfield, P., Christy, J. R., Cuffey, K. M., Dickinson, R. E., … Wallace, J. M. (2000). *Surface temperature reconstructions for the last 2,000 years* (pp. 92–97). New York: The National Academies Press.

Oschmann, W. (2009). Sclerochronology: Editorial. *International Journal of Earth Sciences*, *98*(1), 1–2.

Rayner, N. A., Parker, D. E., Horton, E. B., Folland, C. K., Alexander, L. V., Rowell, D. P., … Kaplan, A. (2003). Global analyses of sea surface temperature, sea ice, and night marine air temperature since the late nineteenth century. *Journal of Geophysical Research*, *108*(D14), 4407. https://doi.org/10.1029/2002JD002670

Reid, P. C., Edwards, M., Beaugrand, G., Skogen, M., & Stevens, D. (2003). Periodic changes in the zooplankton of the North Sea during the twentieth century linked to oceanic inflow. *Fisheries Oceanography*, *12*(4-5), 260–269.

Reynolds, D. J. (2011). *Establishing multi-bivalve species sclerochronology*. Bangor: Bangor University.

Reynolds, D. J., Butler, P. G., Williams, S. M., Scourse, J. D., Richardson, C. A., Wanamaker, A. D., … Sayer, M. D. J. (2013). A multiproxy reconstruction of Hebridean (NW Scotland) spring sea surface temperatures between AD 1805 and 2010. *Palaeogeography Palaeoclimatology Palaeoecology*, *386*, 275–285.

Reynolds, D. J., Richardson, C. A., Scourse, J. D., Butler, P. G., Hollyman, P., Roman-Gonzalez, A., & Hall, I. R. (2017). Reconstructing North Atlantic marine climate variability using an absolutely-dated sclerochronological network. *Palaeogeography Palaeoclimatology Palaeoecology*, *465*, 333–346.

Reynolds, D. J., Scourse, J. D., Halloran, P. R., Nederbragt, A., Wanamaker, A. D., Butler, P. G., … Hall, I. R. (2016). Annually-resolved North Atlantic marine climate over the last millennium. *Nature Communications*, *7*. https://doi.org/10.1038/ncomms13502

Rhein, M., Fischer, J., Smethie, W. M., Smythe-Wright, D., Weiss, R. F., Mertens, C., … Putzka, A. (2002). Labrador Sea Water: Pathways, CFC inventory, and formation rates. *Journal of Physical Oceanography*, *32*(2), 648–665. https://doi.org/10.1175/1520-0485(2002)032

Richardson, A. J., & Schoeman, D. S. (2004). Climate impact on plankton ecosystems in the Northeast Atlantic. *Science*, *305*(5690), 1609–1612.

Richardson, C. A. (2001). Molluscs as archives of environmental change. *Oceanography and Marine Biology*, *39*, 103–164.

Royer, C., Thebault, J., Chauvaud, L., & Olivier, F. (2013). Structural analysis and paleoenvironmental potential of dog cockle shells (*Glycymeris glycymeris*) in Brittany, northwest France. *Palaeogeography Palaeoclimatology Palaeoecology*, *373*, 123–132.

Schöne, B. R. (2013). *Arctica islandica* (Bivalvia): A unique paleoenvironmental archive of the northern North Atlantic Ocean. *Global and Planetary Change*, *111*, 199–225.

Schöne, B. R., Fiebig, J., Pfeiffer, M., Gless, R., Hickson, J., Johnson, A. L. A., … Oschmann, W. (2005, 228). Climate records from a bivalved Methuselah (*Arctica islandica*, Mollusca; Iceland). *Palaeogeography Palaeoclimatology Palaeoecology*, 130–148.

Schöne, B. R., Freyre Castro, A. D., Fiebig, J., Houk, S. D., Oschmann, W., & Kröncke, I. (2004). Sea surface water temperatures over the period 1884–1983 reconstructed from oxygen isotope ratios of a bivalve mollusk shell (*Arctica islandica*, southern North Sea). *Palaeogeography, Palaeoclimatology, Palaeoecology*, *212*(3-4), 215–232.

Schöne, B. R., & Gillikin, D. P. (2013). Unraveling environmental histories from skeletal diaries - advances in sclerochronology. *Palaeogeography Palaeoclimatology Palaeoecology*, *373*, 1–5.

Schöne, B. R., Wanamaker, A. D. Jr., Fiebig, J., Thebault, J., & Kreutz, K. (2011). Annually resolved $\delta^{13}C_{shell}$ chronologies of long-lived bivalve mollusks (*Arctica islandica*) reveal oceanic carbon dynamics in the temperate North Atlantic during recent centuries. *Palaeogeography Palaeoclimatology Palaeoecology*, *302*(1-2), 31–42. https://doi.org/10.1016/j.palaeo.2010.02.002

Scourse, J., Richardson, C., Forsythe, G., Harris, I., Heinemeier, J., Fraser, N., … Jones, P. (2006). First cross-matched floating chronology from the marine fossil record: Data from growth lines of the long-lived bivalve mollusc *Arctica islandica*. *Holocene*, *16*(7), 967–974.

Scourse, J. D., Wanamaker, A. D., Weidman, C., Heinemeier, J., Reimer, P. J., Butler, P. G., … Richardson, C. A. (2012). The marine radiocarbon bomb pulse across the temperate North Atlantic: A compilation of $\Delta^{14}C$ time histories from *Arctica islandica* growth increments. *Radiocarbon*, *54*(02), 165–186. https://doi.org/10.2458/azu_js_rc.v54i2.16026

Sicre, M. A., Hall, I. R., Mignot, J., Khodri, M., Ezat, U., Truong, M. X., … Knudsen, K. L. (2011). Sea surface temperature variability in the subpolar atlantic over the last two millennia. *Paleoceanography*, *26*, PA4218. https://doi.org/10.1029/2011PA002169

Smith, T. M., & Reynolds, R. W. (2004). Improved extended reconstruction of SST (1854–1997). *Journal of Climate*, *17*(12), 2466–2477.

Talley, L. D. (2003). Shallow, intermediate, and deep overturning components of the global heat budget. *Journal of Physical Oceanography*, *33*(3), 530–560. https://doi.org/10.1175/1520-0485(2003)033

Tandon, N. F., & Kushner, P. J. (2015). Does external forcing interfere with the AMOC's influence on North Atlantic Sea surface temperature? *Journal of Climate*, *28*(16), 6309–6323.

Trouet, V., & Van Oldenborgh, G. J. (2013). KNMI climate explorer: A web-based research tool for high-resolution paleoclimatology. *Tree-Ring Research*, *69*(1), 3–13. https://doi.org/10.3959/1536-1098-69.1.3

Urey, H. C. (1948). Oxygen isotopes in nature and in the laboratory. *Science*, *108*(2810), 489–496.

Wanamaker, A. D. Jr., Butler, P. G., Scourse, J. D., Heinemeier, J., Eiriksson, J., Knudsen, K. L., & Richardson, C. A. (2012). Surface changes in the North Atlantic meridional overturning circulation during the last millennium. *Nature Communications*, *3*, 899. https://doi.org/10.1038/ncomms1901

Wanamaker, A. D., Kreutz, K. J., Schöne, B. R., & Introne, D. S. (2011). Gulf of Maine shells reveal changes in seawater temperature seasonality during the Medieval Climate Anomaly and the Little Ice Age. *Palaeogeography, Palaeoclimatology, Palaeoecology*, *302*(1–2), 43–51. https://doi.org/10.1016/j.palaeo.2010.06.005

Wanamaker, A. D., Kreutz, K. J., Schöne, B. R., Maasch, K. A., Pershing, A. J., Borns, H. W., … Feindel, S. (2009). A late Holocene paleoproductivity record in the western Gulf of Maine, USA, inferred from growth histories of the long-lived ocean quahog (*Arctica islandica*). *International Journal of Earth Sciences*, *98*(1), 19–29. https://doi.org/10.1007/s00531-008-0318-z

Witbaard, R., Duineveld, G. C. A., & Dewilde, P. (1997). A long-term growth record derived from *Arctica islandica* (Mollusca, Bivalvia) from the Fladen Ground (northern North Sea). *Journal of the Marine Biological Association of the United Kingdom*, *77*(03), 801–816. https://doi.org/10.1017/S0025315400036201

Witbaard, R., Jansma, E., & Sass Klaassen, U. (2003). Copepods link quahog growth to climate. *Journal of Sea Research*, *50*(1), 77–83.

Witbaard, R., Jenness, M. I., Vanderborg, K., & Ganssen, G. (1994). Verification of annual growth increments in *Arctica islandica* L. from the North Sea by means of oxygen and carbon isotopes. *Netherlands Journal of Sea Research*, *33*(1), 91–101. https://doi.org/10.1016/0077-7579(94)90054-X

Xu, W. D., Miller, P. I., Quartly, G. D., & Pingree, R. D. (2015). Seasonality and interannual variability of the European Slope Current from 20 years of altimeter data compared with in situ measurements. *Remote Sensing of Environment*, *162*, 196–207. https://doi.org/10.1016/j.rse.2015.02.008